SMALL x PHYSICS*

R. KIRSCHNER**

Institut für Theoretische Physik, Universität Leipzig
Augustusplatz 10, D-04109 Leipzig, Germany

(Received September 22, 1995)

Deep-inelastic scattering at small x is a new field of QCD phenomenology which HERA experiments started to explore. The data show the feature expected by the perturbative Regge asymptotics. The aim of the lectures is to give an introduction to the phenomenological and theoretical ideas of small x physics as a preparation to the following lectures at this school. We describe the parton picture of structure function evolution both for increasing Q^2 and for decreasing x and discuss the leading logarithmic approximation of QCD on which this picture is based. The steep rise of the parton density towards smaller x gets saturated by parton recombination. An essential improvement of the leading logarithmic approximation has to be worked out in order to satisfy the unitarity conditions and in this way to describe the parton recombination in perturbative QCD. We introduce the high-energy effective action, discuss reggeization of gluons and the remarkable symmetry properties of the reggeon interractions. Using this symmetry the solution of the BFKL pomeron equation and also the appearence of the pomeron poles are considered in some detail. We outline the construction of the $2 \to 4$ reggeon vertex and of amplitudes which can be used to derive predictions about the hadronic final state.

PACS numbers: 11.55.Jy, 12.38.Lg

---

* Presented at the XXXV Cracow School of Theoretical Physics, Zakopane, Poland, June 4–14, 1995.

** Supported in part by the Volkswagen Stiftung.

1. Deep inelastic scattering at small x

1.1. Structure functions and Regge region

Let us recall the kinematics of deep-inelastic scattering $ep \to eX$, Fig. 1, in particular the relation between the Bjorken variable x to the external momenta. $k_e(k'_e)$ are the four-momenta of the in (out) going lepton and p is the momentum of the proton, the mass of which is denoted by m_p.

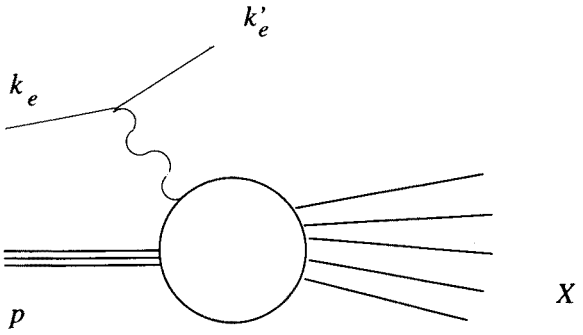

Fig. 1. Kinematics of deep-inelastic scattering.

$$Q^2 = -(k_e - k'_e)^2\,, \qquad \nu m_p = p(k_e - k'_e)\,,$$
$$x = \frac{Q^2}{2\nu m_p}\,, \qquad y = \frac{p(k_e - k'_e)}{p_{k_e}}\,. \tag{1.1}$$

The essential variables are the momentum square of the virtual photon Q^2 and the Bjorken variable x. The square of the invariant mass of the hadronic final state X is given by

$$s = (p + k_e - k'_e)^2 = m_p^2 - Q^2(1 - \tfrac{1}{x})\,. \tag{1.2}$$

The cross section of unpolarised deep-inelastic scattering is written in the following standard form, which is obtained relying on Lorentz, parity and gauge symmetries,

$$\frac{d^2\sigma}{dQ^2\,dx}(x, Q^2, y) = \frac{4\pi\alpha^2}{Q^4}\left[\left(1 - y - \frac{m_p x y}{2pk}\right)\frac{F_2(x, Q^2)}{x} + y^2 F_1(x, Q^2)\right]. \tag{1.3}$$

The structure functions $F_{1/2}(x, Q^2)$ carry essential informations about the dynamics of the interaction of the virtual photon with the proton. This

dynamics can be interpreted as point-like interactions with partons inside the proton. The structure functions are related to the parton densities $q_i(x, Q^2)$,

$$F_2(x, Q^2) = x \sum_i e_i^2 q_i(x, Q^2) . \tag{1.4}$$

Here i runs over all (active) parton types (quark and anti-quark flavours), e_i stands for the electric charge of the parton i.

The parton densities $q_{i/h}(x, Q^2)$ are process independent attributes of the hadron h and enter all cross sections of hard scattering involving h. In QCD the values of the parton densities at arbitrary $Q^2 > m_p^2$ can be calculated from its values at some Q_0^2 by a standard evolution equation.

Hard processes at increasing energies are dominated by parton densities at decreasing x. This strongly motivates the study of the parton densities at small x and shows the significance of the HERA experiments investigating deep-inelastic scattering down to $x \sim 10^{-4}$. Moreover, at small x the standard QCD evolution scheme has to be modifies. Here we enter a new field of QCD phenomenology.

From (1.2) we have at small x the relation $s \approx Q^2/x \gg Q^2$. In this case the virtual Compton amplitude, the forward imaginary part of which determines the cross section (1.3), is in the Regge regime. The large s behaviour of this amplitude, which is determined by the leading Regge singularities, implies the small x behaviour of the parton densities. In particular we have

$$q(x, Q^2) \sim \left(\frac{1}{x}\right)^{\alpha_P(0)} , \qquad \Delta q(x, Q^2) \sim \left(\frac{1}{x}\right)^{\alpha_R(0)} . \tag{1.5}$$

$\alpha_P(0)$ stands for the intercept of the pomeron, *i.e.* the leading singularity in the exchange channel with vacuum quantum numbers, and $\alpha_R(0)$ for the leading singularity in the exchange channel with meson quantum numbers. $\Delta q(x, Q^2)$ stands for a combination of parton densities corresponding to the flavour non-singlet structure functions. Referring to conventional hadron phenomenology [1] one would take the values $\alpha_P(0) = 1.08, \alpha_R(0) = 0.5$.

Because of the large Q^2 in deep-inelastic scattering the situation differs from the usual Regge asymptotics. Q^2 can be choosen large enough to justify the application of perturbative QCD. The perturbative Regge region is characterized by two large momentum scales:

$$s \gg Q^2 \gg m_p^2 . \tag{1.6}$$

In perturbation theory the Regge asymptotics in gauge theories has been investigated in the leading logarithmic approximation. In the case of SU(N) gauge group the leading vacuum channel singularity is located at [2]

$$\alpha_{\mathrm{BFKL}} = 1 + \frac{N \alpha_S}{\pi} 4 \ln 2 . \tag{1.7}$$

With a scale $\kappa \sim 10$ GeV for the running coupling α_S and with $N = 3$ one estimates $\alpha_{\mathrm{BFKL}} \approx 1.5$. In this way one arrives at a prediction for the small x behaviour of the strucure functions much steeper compared to the expectations from conventional hadron phenomenology. The behaviour differs also from the small x asymptotics induced by the usual evolution of parton densities in Q^2 (called r-evolution below).

It is not obvious where the corrections to the leading logarithmic approximation or the non-perturbative contributions become important. The strong increase of the structure function $F_2(x, Q^2)$ with decreasing x observed at HERA [3–5] indicates that the perturbative Regge result (1.7) can be applied in the range of present experiments as a first approximation. The perturbative Regge behaviour shows up not only in the x dependence of the structure functions but also in certain features of the hadronic final state in deep-inelastic scattering. In HERA experiments one is studying for example the transverse energy flux, jet rates at large transverse and longitudinal momenta, and diffractive events, in particular $\gamma^*\rho$ diffraction.

Deep-inelastic scattering at small x is a special case of semi-hard processes, which are characterized by two large momentum scales. Quasi-elastic scattering at relatively large momentum transfer ($s \gg |t| \gg m_p^2$) or inclusive mini-jet production with transverse energy E_T ($s \gg E_T^2 \gg m_p^2$) are other examples, where the perturbative Regge regime applies. There are semi-hard processes of non-Regge type like fragmentation of jets (with energy E_J) at small energy fractions x_E ($E_J \gg x_E E_J \gg m_p$) or at large energy fractions ($E_J \gg (1 - x_E)E_J \gg m_p$). At small $1 - x_E$ large corrections sum up to the Sudakov form factor [6, 7] and at small x_E coherence effects become important, which are appropriately described by angular ordering [8].

1.2. The parton picture

Let us draw the parton picture of the structure function evolution before we discuss some details about how it emerges from QCD.

The parton hit by the virtual photon can be considered as emerging from an evolution starting from the hadron constituents and proceeding by parton radiation. At each step ℓ of the radiation process the transverse momentum κ_ℓ and the longitudinal momentum fraction x_ℓ of the parton change. x is the value of x_ℓ at the final step ($\ell = n$) of the evolution and Q is the upper bound for $|\kappa|$. If x is small then there is room for this process to evolve both in $r = \ln(|\kappa^2|/m_p^2)$ as well as in $y = -\ln x$. The $y - r$ plot Fig. 2 serves as an useful illustration. The features of the evolution in r are well known. At higher steps in this evolution the partons appear in higher multiplicitiy and at higher resolution (a reasonable measure of which

is just r). The new partons cover a negligible fraction of the transverse space occupied by the parent parton.

The evolution in y proceeds without essential changes in the resolution. The new partons appear with about the same size as the parent parton. According to Eq. (2) the multiplicity grows exponentially in y. The partons tend to cover the space inside the proton. The rapid growth of the multiplicity in the first stage of the y-evolution becomes saturated by recombination effects before the partons come too close to each other. The region where the recombination is essential is bounded by the critical line in the $y - r$ plot Fig.2.

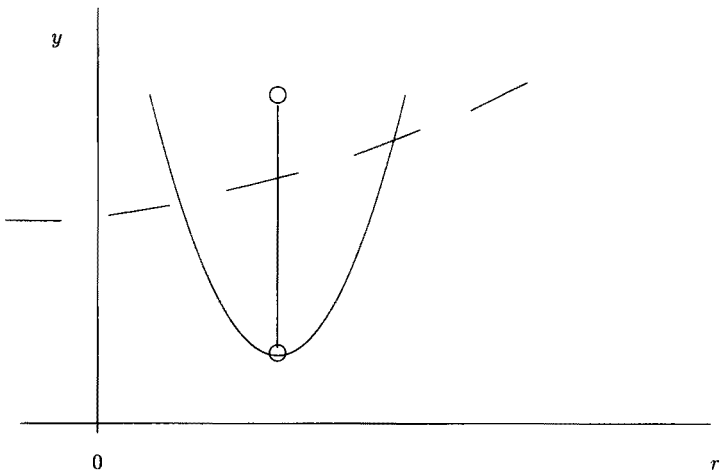

Fig. 2. Parton evolution in r and y. Left to the y axis is the non-perturbative region. The dashed line indicates the critical line and the parabola shows the r range broadening due to the diffusion in the y evolution.

During the evolution in y the value of r undergoes a random walk and may run into the non-perturbative region ($r < 0$). This means in particular that the value of the parton density at given r and y becomes influenced by non-perturbative contributions if y becomes large enough even if r is far from the non-perturbative region.

In both the r-evolution and the y-evolution the process starts with the proton constituents inside the non-perturbative region. Measuring a jet with κ_j, x_j in the hadronic final state one detects an intermediate state of the evolution in the perturbative region (provided κ_j is not small). In the case $x_j \gg x, |\kappa_j^2| \sim Q^2$ this measurement selects a nearly ideal perturbative y-evolution, all features of which are calculable [9].

1.3. The leading logarithmic approximation

In certain kinematical regions large perturbative corrections in each order arise from the integration over κ or x of (real or virtual) partons, if the range in κ is large or if the range in x extends to small values and if the whole range contributes uniformly. In this case the corresponding integrals are approximately of logarithmic form.

In the leading $\ln \kappa^2$ approximation one picks up the logarithmic contributions from the transverse momentum integral of each loop. Graphs with non-logarithmic loops are neglected. Applied to the structure functions at $r > y$ this is the appropriate approximation which can be improved systematically. The leading contribution can be represented as a sum of ladder graphs (in an axial gauge, with propagator and vertex corrections included). There is a strong ordering of the transverse momenta in the loops which leads in particular to trivial transverse momentum integrals. Summing these graphs leads to the known GLAP equation [10]. The iterative structure of the ladders implies in particular the following form of the structure functions, exhibiting their universality.

$$F_2(x,Q^2) = \frac{d\sigma^{\gamma^* j}}{d\hat{t}}|_{\hat{t}=0} \otimes D_{ji}(\frac{x_1}{x_2}, Q^2, Q_0^2) \otimes F_i^{(0)}(x_2, Q_0^2) \qquad (1.8)$$

$\otimes$ abbreviates a convolution integral in the longitudinal momentum fraction. A summation over the parton types i,j is understood. The first factor represents the forward cross section for the virtual photon - parton scattering . Replacing it by other hard scattering cross sections allows to relate the structure functions to distributions in those processes. The second factor represents the r-evolution, the solution of the GLAP equation with the initial distribution $\delta_{ij}\delta(\frac{x_1}{x_2} - 1)$ at Q_0^2.

Because the first two factors are calculable from QCD all experimental information about structure functions and hard processes can be reduced to the distributions $F_i^{(0)}(x, Q_0^2)$ of partons in the hadron at Q_0^2.

In the leading $\ln x$ approximation the integrations over x and κ interchange their roles compared to the above case. For structure functions it is the appropriate approximation at $y > r$. Again the leading contribution can be represented as a sum of ladder graphs, Fig. 3.

Now the lines in the t-channel direction represent reggeized gluons and the interaction is determined by effective vertices. A strong ordering holds now in the longitudinal momenta. More precisely, the loop momenta k_ℓ obey the conditions of multi-Regge kinematics which can be written using the Sudakov decomposition,

$$k = \sqrt{\frac{2}{s}}\ (k_-\ q' + k_+\ p) + \kappa, \qquad q' = q - xp\,, \qquad (1.9)$$

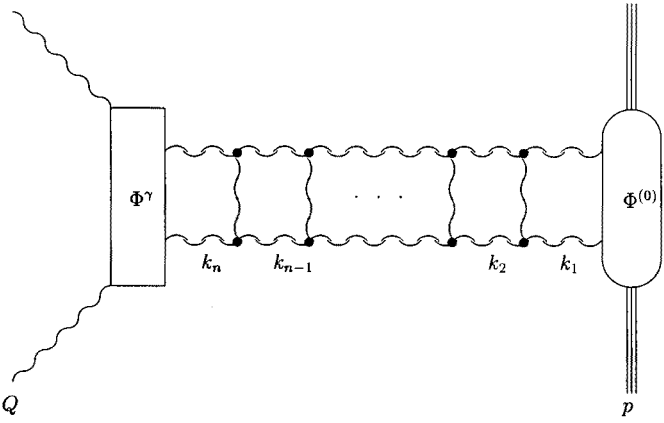

Fig. 3. Gluon ladder graph contributing to the structure function at small x.

(q and p are the 4-momenta of the photon and the proton), in the following form

$$\begin{aligned} k_{+n} \ll \ldots \ll k_{+1}, \qquad & k_{-n} \gg \ldots \gg k_{-1}, \\ k_{+\ell} k_{-\ell} \ll |\kappa_\ell^2|, \qquad & s_\ell \equiv k_{+\ell-1} k_{-\ell+1} \gg |\kappa_\ell^2|, \\ \prod_{\ell=1}^{n} s_\ell = s \prod_{\ell=2}^{n} & |\kappa_\ell - \kappa_{\ell-1}|^2 . \end{aligned} \tag{1.10}$$

The longitudinal momentum integrals become trivial. The iterative structure of the ladders leads to the following form of the resulting structure functions,

$$F_2(x, Q^2) = \Phi^{\gamma *}\Big(\frac{x}{x_1}, Q, \kappa\Big) \otimes \tilde{f}\Big(\frac{x_1}{x_2}, \kappa, \kappa_0\Big) \otimes \Phi^{(0)}(x_2, \kappa_0) . \tag{1.11}$$

Unlike in Eq. (3) here $\otimes$ denotes a transverse momentum integration besides of a trivial x-integral. The universality of the structure functions holds in the y-evolution with this modification. It is also called k_T factorization and its phenomenological relevance has been discussed recently [11]. Here the first factor represents the impact factor coupling (via a quark loop) the virtual photon to the gluon ladder. The second factor describes the y-evolution. Because the first two factors are calculated in QCD the non-trivial information is reduced to the third factor, the hadron impact factor.

The y-evolution is calculated as the solution of the BFKL equation [2, 12], a simple form of which (at vanishing momentum transfer) is given by

$$\frac{\partial}{\partial y} \tilde{f}(y, \kappa, \kappa_0) = \frac{g^2 N}{(2\pi)^3} \int \frac{d^2\kappa'}{|\kappa - \kappa'|^2} \frac{2|\kappa^2|}{|\kappa'^2|} \Big(\tilde{f}(y, \kappa', \kappa_0) - \tfrac{1}{2} \tilde{f}(y, \kappa, \kappa_0) \Big) . \tag{1.12}$$

The asymptotics of the solution at large y,

$$\tilde{f}(y,\kappa,\kappa_0) \sim \frac{|\kappa|}{(2\pi D^2 y)^{1/2}}\, e^{\omega_0 y}\, \exp\left(\frac{-\ln^2(|\kappa^2|/|\kappa_0^2|)}{2D^2 y}\right),$$

$$\omega_0 = \frac{g^2 N}{2\pi^2} 2\ln 2\,, \qquad D^2 = \frac{g^2 N}{\pi^2}\, 7\,\zeta(3)\,, \tag{1.13}$$

exhibits the power-like increase in $\frac{1}{x}$ and the diffusion in r mentioned above.

The critical line, beyond which parton recombination is important, is estimated by using the simple unitarity argument [13] that the $\gamma^* p$ cross section must be bounded by the geometric cross section. This should still be true if γ^* would interact strongly, *i.e.* if $\alpha_{\rm QED}$ is replaced by $\alpha_S(Q^2)$.

$$\frac{\alpha_S(Q^2)}{\alpha_{\rm QED}}\sigma^{\gamma^* p} = \frac{\alpha_S(Q^2)}{Q^2} F_2(x,Q^2) < \pi R_p^2\,. \tag{1.14}$$

Substituting the result of the BFKL equation we obtain the limit of applicability of this equation. Unitarity demands to go beyond the leading logarithmic approximation. A minimal way to improve the unitarity properties of this approximation will be discussed in the following.

Since the publication of the original papers [2, 12] several approaches to the y (BFKL) evolution have been proposed, a modern one will be discussed below. We mention the colour dipole approach to diffractive processes [14] which has attracted much interest recently. The idea of the colour dipole radiation is discussed in the lecture by B.S. Anderson.

There is an equation based on the work by Catani, Ciafaloni, Fiore and Marchesini [15] which interpolates between the r- and the y-evolutions (see also the lecture by J. Kwieciński).

In the case if both the integrals over the longitudinal and over the transverse momenta are approximated by logarithms the calculation becomes a simple exercise. The double logarithmic contributions to the structure functions arise from gluon ladders. Both the contributions to coupling renormalization and to gluon reggeization are single-logarithmic effects. The dominant range of integration over longitudinal and transverse momenta is characterized by the strong ordering conditions

$$\begin{aligned} &x \ll x_n \ll \ldots \ll x_1 \ll 1\,, \\ &Q^2 \gg |\kappa_n|^2 \gg \ldots \gg Q_0^2\,. \end{aligned} \tag{1.15}$$

The sum of ladder graphs is easily calculated.

$$D(x,Q^2) = \sum \left(\frac{n\alpha_S}{\pi}\right)^n \int_x^1 \frac{dx_n}{x_n} \int_{x_n}^1 \frac{dx_{n-1}}{x_{n-1}} \cdots \int_{Q_0^2}^{Q^2} \frac{d\kappa_n^2}{\kappa_n^2} \int_{\kappa_n^2}^{Q^2} \frac{d\kappa_{n-1}^2}{\kappa_{n-1}^2} \cdots$$

$$= \sum \frac{1}{(n!)^2} \left(\frac{N\alpha_S}{\pi} \ln\frac{Q^2}{Q_0^2} \ln\frac{1}{x}\right)^n \sim \exp\left[\left(\frac{N\alpha_S}{\pi} \ln\frac{Q^2}{Q_0^2} \ln\frac{1}{x}\right)^{1/2}\right] \tag{1.16}$$

The following replacement going beyond the double-log accuracy leads to a form compatible with the renormalization group,

$$\frac{\alpha_s}{\pi} \ln\frac{Q^2}{Q_0^2} \to \xi(Q^2,Q_0^2) = \int_{Q_0^2}^{Q^2} \frac{d\kappa^2}{\kappa^2} \frac{\alpha_S(\kappa^2)}{\pi}. \tag{1.17}$$

One should be aware that this is a fairly rough approximation. Nevertheless the result is of interest because it represents the small x asymptotics of the r evolution according to the GLAP equation. We see that (provided that the initial x dependence at Q_0^2 is not steeper) the GLAP equation induces an increase in $y = \ln\frac{1}{x}$ faster that any power of y but less than any power of $\frac{1}{x}$.

Parton density paramentrizations rely on the GLAP equation. One tries to obtain the optimal distributions $q_i(x,Q_0^2)$ describing all data on hard processes. The small x data are well described using an input distribution behaving like (1.5) but with the effective intecept $\alpha_{\text{eff}} = 1.3$ [16]. There is a parametrization approach [17] which manages to describe the rise at small x without assuming a rising initial parton distribution like Eq. (1.5). The point is that the small x asymptotics induced by the GLAP equation $\sim \exp(B(-\ln x)^{1/2})$ can be close to the rise originating from an input distribution like Eq. (1.5) at not too small x by choosing the starting point Q_0^2 correspondingly (actually $B^2 = \frac{4N\alpha_S}{\pi} \ln\frac{Q^2}{Q_0^2}$). However a choice of Q_0 deep in the non-perturbative region which is necessary to describe the data in that way cannot be justified.

In the small-x region a complimentary approach to the parametrization can be considered, relying on the y-evolution Eqs. (1.11)–(1.12) and parametrizing the hadron impact factor $\Phi^{(0)}(x_0,\kappa)$ at some initial $y_0 = \ln\frac{1}{x_0}$ as a function of κ. The behaviour of this impact factor at large κ^2 has to be compatible with the GLAP equation.

Relying on the double-logarithmic approximation one obtains the double scaling behaviour [18] in terms of the variables

$$\sigma = \left(\ln \frac{x_0}{x} \xi(Q^2, Q_0^2)\right)^{1/2}, \rho = \left(\frac{\ln \frac{x_0}{x}}{\xi(Q^2, Q_0^2)}\right)^{1/2} . \tag{1.18}$$

In the lectures by S. Forte it will be shown how corrections can be incorporated and that the present data obey this scaling behaviour.

The r evolution of the structure functions can be well described down to small x by the GLAP equation if the anomalous dimensions or the parton splitting functions are improved by including the sum of terms next-to-leading in Q^2 but leading in the $\ln \frac{1}{x}$ approximation [19].

Both logarithmic approximation schemes discussed above approximate perturbative QCD. It is obvious that improving one of the leading log approximations by corresponding next-to-leading corrections one comes closer to the result of the other approximation scheme in some range of x and Q^2.

1.4. Preasymptotics

Comparing the BFKL behaviour of the deep-inelastic cross section to the behaviour of hadronic cross sections at high energies or — in order to emphasize the contrast — to the real photoproduction cross section questions may arise about the uniqueness of the Regge limit or whether there are two ("soft" and "hard") pomerons. In order to understand the situation one should think of the Regge region as the broad region where

$$s \gg |t|, m_p^2, Q^2 . \tag{1.19}$$

and should not think of the ultimate asymptotics only. The asymptotics is approached gradually by passing through several preasymptotic stages.

In hadron phenomenology this idea allows to understand the data up to present collider energies. A pomeron with the intercept $\alpha_P(0) = 1.08$ fits well the rise of the cross sections, of the central rapidity distribution *etc.* [1]. Unitarity corrections (incorporated by reggeon calculus) ensure that in the asymptotics the Froissart bound is obeyed, $\sigma_{\text{tot}}(s) \sim \ln^2 s$ for $s \to \infty$.

In QCD we have to consider two aspects concerning the preasymptotics. Above we have seen that non-perturbative contributions enter at large y even if Q^2 is not small. Therefore, the perturbative results apply to a preasymptotic stage only. For increasing Q^2 the range in s of this preasymptotics, i.e. the perturbative Regge region, becomes broader.

Within the perturbative Regge region one has to distinguish several subregions. For not too small x the double log behaviour of the GLAP equation still applies before the BFKL behaviour sets in. The power-like

rise in $\frac{1}{x}$ is related to the fact that the leading $\ln x$ approximation does not obey the s-channel unitarity conditions.

It turns out that the unitarity conditions in all sub-energy channels can be saturated by s-channel multi-particle intermediate states which obey the multi-Regge kinematics. This provides the basis for an approach to the next-to-leading $\ln x$ corrections which we call generalized leading logarithmic approximation [22, 23]. It is possible to calculate separately those corrections which improve unitarity. They can be expressed in terms of the multiple exchange of reggeized gluons, where the gluon trajectory and the reggeon interactions are in the first approximation the ones of the leading log approximation (where two reggeons are exchanged). The gluons in the s-channel intermediate states obey the multi Regge kinematics. In some sense the subregions can be related to the typical number of exchanged reggeons.

The remaining next-to-leading $\ln x$ corrections are then accounted for as corrections to the reggeon interactions and to the trajectories [49]. In particular these corrections account for the contributions of s-channel intermediate states with groups of gluons or quarks being not in multi-Regge kinematics, *i.e.* having restricted invariant mass, whereas such groups are separated by large rapiditiy gaps. The latter configuration is called quasi multi-Regge kinematics.

The relation to the operator product expansion and the renormalization group gives a clear prescription for improving the leading $\ln Q^2$ approximation and much work has been done in that direction. In the case of the $\ln x$ approximation only some first steps beyond the leading approximation have been done. The generalized leading $\ln x$ approximation provides a reasonable concept for a systematic improvent of the leading $\ln x$ approximation which will be discussed in some detail in the remaining part of these lectures.

1.5. Regge concepts and notations

The general idea of reggeistics is the separation of scattering and exchange. Depending on the quantum numbers the exchange is universal: It is independent of the scattering particles and (approximately) of the energy $\sqrt{s}$. Deviations from the universality in preasymptotic regions are described by superpositions of contributions with different exchanges.

More technically, the exchanges are related to singularities in the complex angular momentum plane. Simple poles moving with the momentum transfer t correspond to reggeons. Like particles the reggeons are characterized by quantum numbers. Unlike particles there is no spin attributed to them. On the other hand they carry signature, which denotes the parity of the scattering amplitude under the interchange of s and u channels. In

our context it is important that the exchanged gluons and quarks in QCD become reggeons.

We introduce some useful notations.

Consider the scattering amplitude $A(s,t)$ for the process $AB \to A'B'$. Let $\tilde{A}(u,t)$ be the amplitude for the process $A\overline{B}' \to A'\overline{B}$ and introduce the amplitudes of definite signature $\sigma = \pm$,

$$A^{\pm}(s,t) = \tfrac{1}{2}\big(A(s,t) \pm \tilde{A}(u,t)\big)\,. \tag{1.20}$$

The amplitudes $A^{(\sigma)}(s,t)$ are related to their partial waves at large s by

$$A^{(\sigma)}(s,t) = \int\limits_{-i\infty+\delta}^{i\infty+\delta} \frac{d\omega}{2\pi i} f^{(\sigma)}(\omega,t)\left(\frac{s}{M^2}\right)^{1+\omega} \xi_\sigma(\omega)\,. \tag{1.21}$$

M is determined by the momentum transfer t and the masses. $\xi_\sigma(\omega)$ is the signature factor. The transverse vector of the momentum transfer will be denoted by q ($t \approx -|q|^2$). In the case of the virtual Compton amplitude one should not confuse this momentum transfer with the virtualness Q of the photon ($Q^2 = -(k_e - k_e')^2$).

The partial wave of the scattering amplitude can be considered as a sum of multi-reggeon exchange contributions,

$$f^{(\sigma)}(\omega,t) = \sum_{n,m} \Phi_A^{(n)}(\{\kappa_A\}) \otimes f_{n\to m}(\{\kappa_A\},\{\kappa_B\}) \otimes \Phi_B^{(m)}(\{\kappa_B\})\,. \tag{1.22}$$

The impact factor Φ_A describes the coupling of the scattering particle A to n reggeons with transverse momenta $\kappa_{A_1},\ldots,\kappa_{A_n}, \sum \kappa_{A_i} = q$. $f_{n\to m}$ is the $n \to m$ reggeon Green function. $\otimes$ denotes the integration over the transverse momenta $\{\kappa_A\}$ or $\{\kappa_B\}$, respectively. The BFKL pomeron corresponds to the exchange of two reggeized gluons, $n = m = 2$. In this case (1.22) is the same as (1.11).

The vertex connecting the particle A to n reggeons is given by

$$D_A^{(n)}(\omega,\{\kappa_A\}) = \sum_{\ell} \Phi_A^{(\ell)} \otimes f_{\ell\to m}\,. \tag{1.23}$$

2. The multi-Regge effecive action

2.1. General remarks

There are several methods for the investigation of the high-energy behaviour of gauge theories. Conventionally one studies directly the contribution of individual Feynman graphs to the Regge region [20] The Sudakov method (light-cone parametrization of momenta, use of the analytic structure for calculating the longitudinal momentum integrals) is appropriate for evaluating the asymptotics of graphs [21]. The construction of higher order amplitudes from multiparticle amplitudes of lower order by unitarity is a powerful approach [22, 23, 25, 35]. Some results have been obtained or checked by starting from the corresponding string amplitudes and taking the limit of vanishing string tension [30, 31]. White proposed [24] to work with a reggeon calculus with coloured odd-signature reggeons.

The methods mentioned work successfully in the leading logarithmic approximation. Lipatov has proposed [26] to use the multi-Regge effective action, which summarises the leading log results in a simple form, as a starting point for a systematic improvement of this approximation.

The effective action can be obtained from the effective vertices of scattering and production by inventing convenient fields descibing scattering or exchanged gluons (and quarks). The effective vertices take a particular simple form in the helicity basis and in complex notations for the transverse vectors. In the leading log approximation these vertices can be read off from multi-particle tree amplitudes. The latter can be obtained from elastic amplitudes by t-channel unitarity [26] or from corresponding string amplitudes [30, 31].

There is an approach [27] which relates the effective action directly to the original QCD action. One starts formally from the functional integral where redundant field components have been eliminated. The essential step is the separation of modes with respect to the multi-Regge kinematics. The "heavy" momentum modes which correspond neither to scattering nor to exchanged particles in this kinematics are integrated out approximately. In the following we outline the main steps of this approach for the case of SU(N) gauge theory without quarks.

2.2. Eliminating redundant field components

We start from the Yang–Mills action and impose the ligh-cone axial gauge condition $A_- = 0$. We describe the two longitudinal projections of a vector by light-cone components and the transverse projections by complex numbers,

$$A_\pm = A_0 \pm A_3, A = A^1 + iA^2, A^* = A^1 - iA^2 . \qquad (2.1)$$

This convention will be adopted for the vector potential A^μ, for momentum vectors k^μ and positions x^μ. For the derivatives with respect to the coordinates the definition is slightly modified in order to obey the relations

$$\partial_+ x_- = \partial_- x_+ = \partial x = \partial^* x^* = 1 . \tag{2.2}$$

In the gauge $A_- = 0$ the component A_+ enters the action only in first and second power and therefore can be integrated out exactly. The result can be written in terms of currents

$$\begin{aligned} J^a_- &= i(A^* T^a \overleftrightarrow{\partial}_- A), \quad j^a = (A^+ T^a A), \\ J^{a*} &= i(A^* T^a \overleftrightarrow{\partial} A), \quad J^a = i(A^* T^a \overleftrightarrow{\partial}^* A), \end{aligned} \tag{2.3}$$

and the field combinations

$$\mathcal{A}_+ = \partial_-^{-1}(\partial A + \partial^* A^*), \quad \mathcal{A}' = i(\partial A - \partial^* A^*) . \tag{2.4}$$

We shall use the abbreviation

$$(AT^a B) = -if^{abc} A^b B^c . \tag{2.5}$$

f^{abc} are the structure constants of SU(N).

$$\begin{aligned} \mathcal{L} &= \mathcal{L}^{(2)} + \mathcal{L}^{(3)} + \mathcal{L}^{(4)}, \\ \mathcal{L}^{(2)} &= -2A^{a*}(\partial_+\partial_- - \partial\partial^*)A^a, \\ \mathcal{L}^{(3)} &= -\frac{g}{2} J^a_- \mathcal{A}^a_+ - \frac{g}{2} j^a \mathcal{A}'^a, \\ \mathcal{L}^{(4)} &= \frac{g^2}{8} J^a_- \partial_-^{-2} J^a_- - \frac{g^2}{8} j^a j^a . \end{aligned} \tag{2.6}$$

The meaning of the non-local operator ∂_-^{-1} is to be specified. However the region of very small longitudinal momenta will not be important in our analysis.

With the elimination of redundant field components we have prepared the action for the next step. The separation of modes would be ambiguous under arbitrary gauge transformations.

2.3. Separation of modes

We consider once more the conditions of multi-Regge kinematics (1.10). If the momenta k_i of the s-channel particles are close to mass shell then from

the strong ordering of the longitudinal momenta follows that the momentum transfer vectors are essentailly transverse,

$$q_j = p_A - \sum_{i=1}^{j} k_{i-1}\,, \quad q_{j+}q_{j-} \ll |q_j|^2\,. \tag{2.7}$$

This characterizes the typical momentum range of the exchanged particles. It motivates us to separate the modes of the field A in the following way,

$$\begin{aligned} &A \to A_t + A_s + A_1\,,\\ &A_t : |k_+k_-| \ll |\kappa|^2\,,\\ &A_s : |k_+k_- - |\kappa|^2| \ll |\kappa|^2\,,\\ &A_1 : |k_+k_-| \gg |\kappa|^2\,. \end{aligned} \tag{2.8}$$

A_t denotes the modes of the exchanged gluons and A_s the ones of scattering gluons. The "heavy" modes A_1 are to be integrated out approximately. The subscripts will be omitted in the final expressions after introducing appropriate notations.

Introducing the separation of modes into the action each term splits off into a number of terms. We obain separate kinetic terms for each A_t, A_s, A_1. In order to analyse the triple terms resulting from $\mathcal{L}^{(3)}$ we consider first their contribution to the scattering of a gluon with large k_- and then the scattering with large k_+.

The contribution of $\mathcal{L}^{(3)}$ where two fields are of types A_s or A_t carrying large k_- ($\tilde{A} = A_s + A_1$) and one field is of type A_t or A_s with relatively small k_- can be written as

$$\mathcal{L}^{(3+)} = -\frac{g}{2}\tilde{J}^a_-\tilde{A}^a_+ - g\tilde{j}^a\tilde{A}'^a + \frac{g}{2}(\tilde{J}^a\tilde{A}^{a*} + \tilde{J}^{a*}\tilde{A}^a) + \mathcal{O}(k_-^{-1})\,. \tag{2.9}$$

The first term gives a contribution to scattering of order k_-, the next two terms of order k_-^0. The first term is just the leading effective scattering vertex for gluons with large k_-, if we restrict the fields in $\tilde{J}_-$ to A_s and the fields in $\tilde{A}_+$ to A_t. As we shall see the first term also contributes to the effective production vertex and is the relevant term for the approximate integration over "heavy" modes. The next two terms become important if one studies the corrections suppressed by one power of s, or equivalently, the Regge singularities in the vicinity of angular momentum $j = 0$.

Now we pick up the terms in $\mathcal{L}^{(3)}$ which are relevant for the scattering with large k_+. This are the terms where two fields are of type $A_s + A_1 = \tilde{A}$ carrying large k_+ and one field of type A_t. The latter should carry k_- of

the same order as the largest k_- of the first two fields. We split the result into two parts, $\mathcal{L}^{(3-)} = \mathcal{L}^{(3-,1)} + \mathcal{L}^{(3-,2)}$, where

$$\mathcal{L}^{(3-,2)} = ig\partial_- A_t^a(\tilde{A}^* T^a \partial_-^{-1}(\partial\tilde{A} + \partial^*\tilde{A}^*)) + igA_t^a(\tilde{A}^* T^a \partial\tilde{A}) + \text{c.c.} \quad (2.10)$$

Contracting this vertex $\mathcal{L}^{(3-)}$ with $\mathcal{L}^{(3+)}$ (with the exchange of A_t) we obtain lowest order contributions to the high-energy $2 \to 2$ scattering. Also $\mathcal{L}^{(4)}$ contributes to scattering. It turns out that the latter contributions are cancelled from the ones from $\mathcal{L}^{(3-,1)}$. $\mathcal{L}^{(3-,2)}$ contributes to the effective scattering vertex for gluons with large k_+.

2.4. Integration over "heavy" modes

We assume that the fluctuations A_1 are small and linearize $\mathcal{L}^{(2)} + \mathcal{L}^{(3+)}$ in A_1. At small coupling the integration over A_1 is dominated by the saddle point determined by the equation obtained from the latter part of the action ($\tilde{A} = A_s + A_t$),

$$-2\partial_+\partial_- A_1^a + \frac{ig}{2}(\tilde{A}_+ T^a \partial_- A_s) = 0\,. \quad (2.11)$$

With the solution $A^{(0)}$ we obtain the following quartic term in the action,

$$2A_1^{(0)*}\partial_+\partial_- A_1^{(0)} = -\frac{g^2}{8}(A_s^* T^a \overleftrightarrow{\partial}_- A_s)(\partial_+^{-1}\tilde{A}_+ T^a \tilde{A}_+)\,. \quad (2.12)$$

The first factor is proportional to J_-. Therefore, it is natural to interprete the result as induced by $\mathcal{L}^{(2)} + \mathcal{L}^{(3+)}$ and the induced triple vertex

$$\mathcal{L}_{\text{ind}}^{(1)} = \tfrac{ig}{2}\partial\partial^*\mathcal{A}_-^a\left(\partial_+^{-1}\tilde{A}_+ T^a \tilde{A}_+\right),$$
$$\mathcal{A}_- = \tfrac{1}{2}\partial_-(\partial\partial^*)^{-1}(\partial A_t + \partial^* A_t^*)\,, \quad (2.13)$$

The induced vertex is essential for obtaining the effective vertices of production and of scattering with large k_+.

At the first sight $\mathcal{A}_+$ and $\mathcal{A}_-$ seem to be not independent. However the cancellation of the contribution of $\mathcal{L}^{(3-,1)}$ against $\mathcal{L}^{(4)}$ means also that $\mathcal{A}_+$ couples to particles with large k_- whereas $\mathcal{A}_-$ couples to particles with large k_+. In this way as a reflection of the multi-Regge ordering of longitudinal momenta the t-channel exchange aquires an orientation along the rapidity axis.

2.5. The effective vertices

We write the contribution $\mathcal{L}_{\rm ind}^{(-+)}$ of the induces vertex $\mathcal{L}_{\rm ind}^{1}$ (2.13) for the case where one $\tilde{\mathcal{A}}_t$ is restricted to A_t and one to A_s. For the latter we substitute $\mathcal{A}_+^{(s)} = \partial_-^{-1}(\partial A_s + \partial^* A_s^*)$. Likewise we write the contribution $\mathcal{L}^{(3-+)}$ of the leading term in $\mathcal{L}^{(3+)}$ for the case if $\tilde{\mathcal{A}}_+$ is restricted to the modes A_t and one field in J_- is restricted to A_s and the other to A_t.We substitute here A_t in terms of $\mathcal{A}_-$ (2.13). The sum of both contributions yields the effective vertex of gluon production,

$$\mathcal{L}_p = \mathcal{L}_{\rm ind}^{(-+)} + \mathcal{L}^{(3-+)} = ig\,(\partial^* \mathcal{A}_- T^a \partial \mathcal{A}_+)\,\partial^{-1} A_s^{a*} + \text{c.c.} \tag{2.14}$$

The non-locality can be shifted from the effective production vertex into the kinetic term by substituting

$$A_s = i\partial^* \phi\,. \tag{2.15}$$

Now we write the contribution $\mathcal{L}_{\rm ind}^{(-)}$ of the induced vertex $\mathcal{L}_{\rm ind}^{(1)}$ (2.13) for the case where both $\tilde{\mathcal{A}}_+$ are restricted to modes A_s and substitute $\mathcal{A}_+^{(s)} = \partial_-^{-1}(\partial A_s + \partial^* A_s^*)$. Also from $\mathcal{L}^{(3-,2)}$ we write the contribution where $\tilde{A}$ are restricted to A_s. Here we express A_t in terms of $\mathcal{A}_-$ (2.13). The sum of both contributions is the effective scattering vertex of gluons with large k_+,

$$\mathcal{L}_s^{(-)} = \mathcal{L}^{(3-,2)} + \mathcal{L}_{ind}^{(-)} = \frac{ig}{2}\left(\frac{\partial^*}{\partial} A^* T^a \overleftrightarrow{\partial} + \frac{\partial}{\partial^*} A\right) \mathcal{A}_-^a\,. \tag{2.16}$$

This is to be compared with the effective scattering vertex for gluons with large k_-, i.e. the first term of $\mathcal{L}^{(3+)}$ (2.9),

$$\mathcal{L}_s^{(+)} = \frac{ig}{2}(A^* T^a \overleftrightarrow{\partial}_- A)\mathcal{A}_+^a\,. \tag{2.17}$$

The vertex $\mathcal{L}_s^{(-)}$ is obtained from the vertex $\mathcal{L}_s^{(+)}$ by interchanging the indices $+$ and $-$ and by replacing

$$A \to \frac{\partial^*}{\partial} A^*\,, \tag{2.18}$$

which is just the gauge transformation leading from the gauge $A_- = 0$ to the gauge $A_+ = 0$. Also regarding this gauge relation it is natural to represent the scattering gluons by the complex scalar ϕ (2.15).

Besides of the considered contributions the induced vertex involves still the case $\mathcal{L}_t$ where all three fields are in the modes A_t of exchanged fields.

2.6. The effective action for gluons

The multi-Regge effective action for gluons is given by

$$\begin{aligned}
\mathcal{L} &= \mathcal{L}_{kin} + \mathcal{L}_s + \mathcal{L}_p + \mathcal{L}_t, \\
\mathcal{L}_{\text{kin}} &= -\tfrac{1}{2}(\partial^*\phi^a)\Box(\partial\phi^{a*}) - 2\mathcal{A}_+^a\partial\partial^*\mathcal{A}_-^a, \\
\mathcal{L}_s &= -\frac{ig}{2}(\partial\phi^* T^a \overleftrightarrow{\partial}_- \partial^*\phi)\mathcal{A}_+^a + \frac{ig}{2}(\partial^*\phi^* T^a \overleftrightarrow{\partial}_+ \partial\phi)A_-^a, \\
\mathcal{L}_p &= g\phi^a(\partial\mathcal{A}_- T^a \partial^*\mathcal{A}_+) + g\phi^{a*}(\partial^*\mathcal{A}_- T^a \partial\mathcal{A}_+), \\
\mathcal{L}_t &= \frac{ig}{2}\partial\partial^*\mathcal{A}_-^a(\partial_+^{-1}\mathcal{A}_+ T^a \mathcal{A}_+) + \frac{ig}{2}\partial\partial^*\mathcal{A}_+^a(\partial_-^{-1}\mathcal{A}_- T^a \mathcal{A}_-). \qquad (2.19)
\end{aligned}$$

The non-local operator Ω suppresses the propagation of modes of ϕ which are outside the vicinity of the mass shell, $|k_+k_- - |\kappa|^2| \ll |\kappa|^2$. Likewise Y suppresses the propagation of modes of $\mathcal{A}_\pm$ which are not in the range appropriate for exchanged particles, $|k_+k_-| \ll |\kappa|^2$. The effective vertices are represented by the graphs Fig. 4.

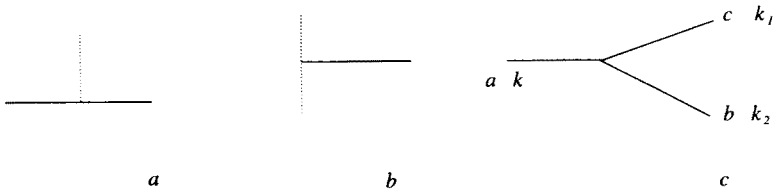

Fig. 4. Vertices of the effective action. a — Effective vertex of emission; b — effective vertex of scattering; c — triple vertex of exchanged gluons.

The result (2.19) has been extended to QCD with quarks included. Massless spinor fields ψ are decomposed into light-cone components $\psi_\pm = \frac{1}{4}\gamma_\pm\gamma_\mp\psi$. In the gauge $A_- = 0$ the component ψ_+ decouples. The separation of modes is introduced in analogy to (2.8), $\psi_- \to \psi_{1-} + \psi_{s-} + \psi_{t-}$. In the effective action the scattering quarks are represented by two complex fields χ_-, χ_-^*, where $\partial\chi_-, \partial^*\chi_-^*$ are components of ψ_{s-} in a standard basis. The exchanged fermions are described by the complex fields $a_\pm, a_\pm^*$ which are related to the components of ψ_t in the same basis. The fermion exchange depends on the transferred helicity.

The exchanged quarks and gluons behave like reggeons. The triple vertex of exchanged gluons $\mathcal{L}_t$ carries the essential features of White's triple vertex of odd-signature reggeons [24, 34].

There are supersymmetry relations between the fermionic and the gluonic effective vertices, which hold if one replaces the fundamental representation of the quarks by the adjoint one. Further there are Weizsäcker–Williams type relations between the effective vertices of scattering and production. The effective action shows a separation of longitudinal and transverse subspaces. The interaction terms are symmetric separately with repect to dilatations and Lorentz boosts or rotations in these subspaces.

The substitution (2.15) of A_s by ϕ erases the traces of the initial gauge choice. There is no doubt about the gauge indenpendence in the considered approximation because there is a derivation operating merely with amplitudes on mass shell [26].

A gauge symmetric appraoch has been proposed recently [29]. The gauge potentials in the axial gauge A_σ and the ones in an arbitrary gauge V_μ are related by

$$\begin{aligned} A_\sigma(x) &= U_-^{-1}[V](x)(V_\sigma + \frac{i}{g}\partial_\sigma)U_-[V](x)\,, \\ U_-[V](x) &= P\exp[-ig\int_{-\infty}^{x_+} dx_+ V_-]\,. \end{aligned} \tag{2.20}$$

Consider the effective action without the production vertices $\mathcal{L}_p$ and the triple vertices of exchanged gluons $\mathcal{L}_t$. The exchanged fields $\mathcal{A}_\pm$ enter this truncated action bilinear and can be eliminated by using the equations of motion. For example, by variation with respect to $\mathcal{A}_+$ we obtain

$$4\partial\partial^*\mathcal{A}_- = gJ_-[A]\,. \tag{2.21}$$

Both sides can be expressed in terms of V_μ.

$$\begin{aligned} J_-[A] &= U_-^{-1}[V]J_-[V]U_-[V]\,, \\ \mathcal{A}_- &\approx -\frac{i}{g}\partial_- U_-[V]\,. \end{aligned} \tag{2.22}$$

Elimiating $\mathcal{A}_\pm$ we obtain the current-current interaction,

$$J_-[A](\partial\partial^*)^{-1}J_+[V]\,.$$

We express this vertex in terms of V_μ by using (2.22) and the equations of motion (2.21) (and the analogous equation for J_+) and obtain

$$\mathcal{L}_s \to \mathrm{tr}(\partial_-\partial U_-[V]\ \partial_+\partial^* U_+[V])\,. \tag{2.23}$$

In the case of quasi-elastic scattering the scattering particles can be described by Wilson lines, *i.e.* path-ordered exponentials of the type $U_{\pm}[V]$. Then one can restrict the action to (2.23). In this approximation we have classically $\partial_+\partial_- U_{\pm}[V] = 0$. This allows to do the integrals over the longitudinal coordinates in the action. One arrives at a two-dimensional σ model and reproduces in this way the effective action by E. and H. Verlinde [32].

3. Reggeization and reggeon interactions

3.1. Reggeization of gluons

We consider the high-energy behaviour of an odd signature amplitude with gauge group octet exchange (A) and use the partial wave representation (1.21), (1.22) in terms of impact factors and (reggeon) exchange Green function. In lowest order we have one-gluon exchange and the corresponding Green function is

$$f_A^{(0)}(\omega, q) = \frac{|q|^2}{\omega}. \tag{3.1}$$

The triple vertices of exchanged gluons $\mathcal{L}_t$ give rise to self-energy type graphs (Fig. 5a),

$$-\frac{g^2 N}{2(2\pi)^4} \int \frac{d^4k |q|^4}{k_+ k_- |\kappa|^2 |q-\kappa|^2}. \tag{3.2}$$

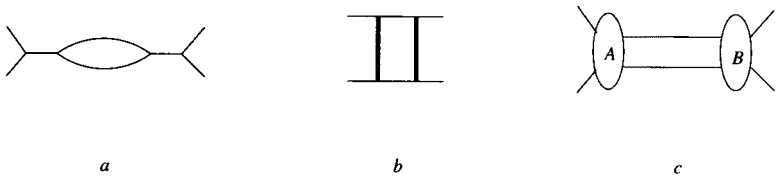

a *b* *c*

Fig. 5. Reggeization. Interpretation of the longitudinal momentum integral.

The range of integration over $k_{\pm}$ has to be defined by taking the dumping factors Y in the propagators into account. We recall that $\mathcal{L}_t$ arised from the heavy mode intermediate states. Therefore the graph of Fig.5a can be interpreted as the one in Fig. 5b, where the heavy lines represent the heavy modes. This is reminicent of a two reggeon exchange graph, Fig. 5c. However the heavy mode intermediate states do not correspond to impact factors with normal analytic properties. Including the intermediate states of gluons close to mass shell the analytic properties are restored and the graph Fig. 5a can be evaluated as a reggeon diagram, i.e. referring to Fig. 5c and

using the dispersion relations for the impact factors A and B. This gives a definite prescription for evaluating the longitudinal momentum integral,

$$-\frac{g^2N}{2(2\pi)^4}\frac{s}{2}\int\frac{dk_+dk_-d^2\kappa|q|^4}{[(p_A-k)^2+i\epsilon][(p_B+k)^2+i\epsilon]|\kappa|^2|q-\kappa|^2}\,. \tag{3.3}$$

Now the intergral over k_+ is done by taking the residue in one of the poles. The integral over k_- then yields the necessary logarithm of s,

$$-\frac{g^2N}{2(2\pi)^3}\ln\frac{s}{|q|^2}\int\frac{d^2\kappa|q|^4}{|\kappa|^2|q-\kappa|^2}\,. \tag{3.4}$$

In the partial wave representation (1.21)–(1.22) this result corresponds to the following contribution to the exchange Green function,

$$\frac{1}{\omega^2}(-g^2N)|q|^2\alpha_G(q)\,, \tag{3.5}$$

where $\alpha_G(q)$ is the gluon trajectory integral,

$$\alpha_G(q)=\frac{1}{2(2\pi)^3}\int\frac{d^2\kappa|q|^4}{|\kappa|^2|q-\kappa|^2}\,, \tag{3.6}$$

which has to be defined e.g. by dimensional regularization. The gluon trajectory is $1-g^2N\alpha_G(q)$.

The sum of all loops of the considered type results in the exchange Green function of one reggeized gluon,

$$f_A(\omega,q)=\frac{|q|^2}{\omega+g^2N\alpha_G(q)}\,. \tag{3.7}$$

The derivation of the gluon reggeization relies on the vertex $\mathcal{L}_t$ and includes contributions from $\mathcal{L}_p$ in specifying the longitudinal momentum intergrals. Some doubts could arise, whether we have accounted for all contributions in the leading log approximation correctly. Therefore we perform a consistency check and show that the exchange of two reggeized gluons in the channel with the quantum numbers of one gluon by summing over all interactions via $\mathcal{L}_p$ results again in the Regge singularity of one reggeized gluon. This result is one aspect of the important reggeon bootstrap property.

The momenta of the scattering gluons are restricted to be close to mass shell. Relaxing this condition the vertex $\mathcal{L}_p$ represents all interactions of the exchanged gluons. Indeed, in this case there is no room left for the heavy mode contribution resulting in $\mathcal{L}_t$. Since the parameter defining the

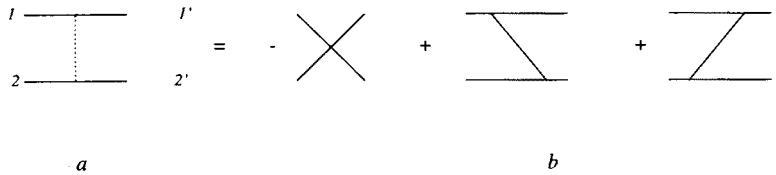

a b

Fig. 6. The transition kernel $2 \to 2$ in s-channel — a, and t-channel — b representations.

closeness to the mass shell does not enter the final result we should be able to reproduce it relying on $\mathcal{L}_p$ only.

The exchange of two reggeized gluons without interaction (Mandelstam cut) corresponds to the following Green function ($\kappa_1 + \kappa_2 = q$),

$$f^{(0)}_{2,A}(\omega, \kappa_1, \kappa_2, \overline{\kappa}_1, \overline{\kappa}_2) = \frac{|\kappa_1|^2 |\kappa_2|^2 \delta(\kappa_1 - \overline{\kappa}_1)\delta(\kappa_2 - \overline{\kappa}_2)}{\omega + g^2 N \alpha_G(\kappa_1) + g^2 N \alpha_G(\kappa_2)}. \tag{3.8}$$

The vertices $\mathcal{L}_p$ lead to the interaction Fig. 6a. The transverse momentum factors corresponding to this graph (two vertices of type $\mathcal{L}_p$ and the ϕ propagator) are given by

$$K_{2\to 2}(\kappa_1, \kappa_2, \kappa_1', \kappa_2') = \frac{\kappa_1 \kappa_1'^* \kappa_2^* \kappa_2' + \text{c.c.}}{|\kappa_1 - \kappa_1'|^2}. \tag{3.9}$$

The sum of all interactions of this type is obtained as the solution of the following integral equation,

$$\tilde{f}_{2,A}(\omega, \kappa_1, \kappa_2) = \frac{1}{\omega + g^2 N \alpha_G(\kappa_1) + g^2 N \alpha_G(\kappa_2)}$$

$$\times \left(1 + \frac{g^2 N}{2(2\pi)^3} \int \frac{d^2\kappa_1' d^2\kappa_2'}{|\kappa_1' \kappa_2'|^2} K_{2\to 2}(\kappa_1, \kappa_2, \kappa_1', \kappa_2') \tilde{f}_{2,A}(\omega, \kappa_1', \kappa_2')\right). \tag{3.10}$$

For simplicity we wrote the equation for the Green function convoluted with one impact factor, $\tilde{f} = f \otimes \Phi_B$ with $\Phi_B = 1$. The result for the Green function of two reggeized gluons with all interactions in the channel with single gluon quantum numbers is given by

$$f_{2,A}(\omega, \kappa_1, \kappa_2; \overline{\kappa}_1, \overline{\kappa}_2) = \delta(\kappa_1 - \overline{\kappa}_1)\delta(\kappa_2 - \overline{\kappa}_2) \frac{|\kappa_1|^2 |\kappa_2|^2}{\omega + g^2 N \alpha_G(\kappa_1 + \kappa_2)}. \tag{3.11}$$

We find the same Regge pole in ω as for one reggeized gluon according to the reggeon bootstrap.

3.2. Multi-reggeon exchange

Now we consider the positive-signature gauge group singlet channel, which is relevant in particular for the structure functions. The minimal number of exchanged gluons in this channel is two. The interaction between the exchanged gluons is given by the vertices $\mathcal{L}_p$ and $\mathcal{L}_t$. Since their contributions corresponds to complementary longitudinal momentum ranges (close and far from mass shell) and since the result does not depend on the parameter dividing these regions the transverse momentum dependence of the interaction can be described equally well by either $\mathcal{L}_p$ or $\mathcal{L}_t$.

The transverse momentum kernel of the two reggeized gluon interaction does not depend on the gauge group quantum numbers. It has been obtained above as the product of two vertices $\mathcal{L}_p$. Alternatively one can obtain this kernel by a t-channel approach starting from $\mathcal{L}_t$ [33, 34]. The contribution of 3 intermediate exchanged gluons to the $2 \to 2$ reggeon Green function is given by the last two graphs in Fig. 6b. A condition following from the Ward identity leads one to add the quartic vertex $(\mathcal{A}_-\mathcal{A}_-\mathcal{A}_+\mathcal{A}_+)$ represented by the first graph in Fig. 6b. In general this condition requires the Green function of reggeized gluons to vanish together with any of the transverse momenta. The graphs Fig. 6b stand for the expression (in the same sequence)

$$K_{2\to 2}(\kappa_1, \kappa_2; \kappa_1', \kappa_2') = -|\kappa_1 + \kappa_2|^2 + \frac{|\kappa_1|^2|\kappa_2'|^2 + |\kappa_2|^2|\kappa_1'|^2}{|\kappa_1 - \kappa_1'|^2}. \quad (3.12)$$

It is not difficult to check the coincidence of the expressions (3.9) and (3.12).

Now we go a step beyond the leading logarithmic approximation and consider the exchange of an arbitrary number of gluons. We assume here that the number of reggeized gluons in all t-channel intermediate states is the same. The situation of a changing number of reggeons will be discussed below in Section 4.3. According to the concept of the generalized leading log approximation these reggeized gluons interact pairwise via $K_{2\to 2}$ and

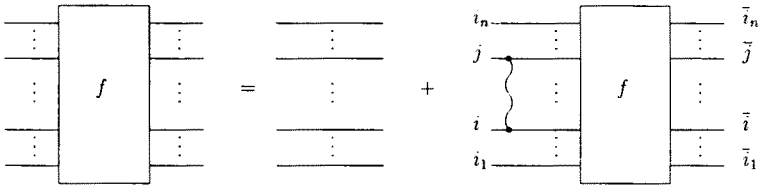

Fig. 7. Equation for the n-reggeon Green function.

their trajectory is determined by $\alpha_G(\kappa)$ as in the leading log approximation. Therefore the $n \to n$ reggeon Green function obeys the equation (Fig. 7),

$$f_{n\to n}(\omega;\{\kappa_\ell\},\{\overline{\kappa}_\ell\}) = [\omega + g^2 N \sum \alpha_G(\kappa_\ell)]^{-1}$$
$$\Big(\prod |\kappa_\ell|^2 \delta(\kappa_\ell - \overline{\kappa}_\ell) + \sum_{i<j} (T_i \otimes T_j)\mathcal{H}^{(0)}_{ij} \otimes f_{n\to n}\Big)\,. \tag{3.13}$$

The interaction is described by the kernel $K_{2\to 2}$,

$$\mathcal{H}^{(0)}_{12} \otimes f_{n\to n}(\omega;\{\kappa_\ell\},\{\overline{\kappa}_\ell\}) = \frac{g^2}{(2\pi)^3}\int \frac{d^2\kappa_1' d^2\kappa_2'}{|\kappa_1'|^2|\kappa_2'|^2}$$
$$K_{2\to 2}(\kappa_1,\kappa_2;\kappa_1',\kappa_2') f_{2\to 2}(\omega,\kappa_1',\kappa_2')\,. \tag{3.14}$$

The latter integral as well as the trajectory integral $\alpha_G(q)$ involve infrared divergencies. In the gauge-group singlet channel these divergencies cancel. In this case we multiply both sides of (3.13) by the inverse of the n-reggeon propagator $(\omega + g^2 N \sum \alpha_G(\kappa_\ell))$ and combine the terms proportional to $\alpha_G(\kappa)$ with the interaction kernel $K_{2\to 2}$ in such a way that the result defines a finite operator.

To show how this works in detail, we write the gauge group structure explicitely. Let $\{a_\ell\},\{\bar{a}_\ell\}$ be the gauge group indices of the n incoming (left side in Fig. 7) and n outgoing reggeized gluons in $f_{n\to n}$.

$$((T_1 \otimes T_2)f)_{\{a_\ell\},\{\bar{a}_\ell\}} = T^a_{a_1 a_1'} T^a_{a_2 a_2'} \prod_3^n \delta_{a_\ell a_\ell'} f_{\{a_\ell'\},\{\bar{a}_\ell\}}\,. \tag{3.15}$$

The condition of singlet exchange means that an arbitrary group transformation acting on the incoming indices $\{a_\ell\}$ only does not change the Green function. For a small transformation the second order in the transformation parameter gives

$$\sum_{i\neq j}(T_i \otimes T_j)f + \sum_i (T_i \otimes T_i)f = 0\,,$$
$$((T_1 \otimes T_1)f)_{\{a_\ell\},\{\bar{a}_\ell\}} = T^a_{a_1 b} T^a_{b a_1'} \prod_2^n \delta_{a_\ell a_\ell'} f_{\{a_\ell'\},\{\bar{a}_\ell\}}$$
$$= N f_{\{a_\ell\},\{\bar{a}_\ell\}}\,. \tag{3.16}$$

The latter relation allows to write the equation as

$$\omega f_{n\to n} = \prod |\kappa_\ell|^2 \delta(\kappa_\ell - \overline{\kappa}_\ell) + \sum_{i<j}(T_i \otimes T_j)\mathcal{H}_{ij} \otimes f_{n\to n}\,, \tag{3.17}$$

where the integral kernel defining the finite operator $\mathcal{H}_{12}$ is given by

$$\mathcal{H}_{12}(\kappa_1,\kappa_2;\kappa_1',\kappa_2') = K_{2\to 2}(\kappa_1,\kappa_2,\kappa_1',\kappa_2') - \delta(\kappa_1-\kappa_1')|\kappa_1|^2\alpha_G(\kappa_1) - \delta(\kappa_2-\kappa_2')|\kappa_2|^2\alpha_G(\kappa_2)\,. \tag{3.18}$$

3.3. Conformal symmetry and factorizability

We change to the impact parameter representation by Fourier transformation with respect to the transverse momenta. The two-reggeon interaction is now represented by an operator acting on the transformed partial wave being now a function of the impact parameters $x_\ell, \ell = 1,...,r$. The operator is obtained from (3.18) by applying the substitutions

$$\kappa_1 \to \partial_1^*\,, \quad \kappa_2^* \to \partial_2\,,$$
$$|\kappa_1-\kappa_1'|^{-2} \to -\ln|x_{12}|^2\,, \quad \alpha_G(\kappa_1) \to -\ln(\partial_1\partial_1^*) + \psi(1)\,. \tag{3.19}$$

∂_1 is the differentiation with respect to x_1, $-\psi(1)$ is the Euler–Mascheroni number and $x_{12} = x_1 - x_2$.

It is remarkable that the resulting operator decomposes into a holomorphic and an antiholomorphic part.

$$\hat{\mathcal{H}}_{GG} = H_G + H_G^*,$$
$$H_G = 2\psi(1) - \partial_1^{-1}\ln x_{12}\partial_1 - \partial_2^{-1}\ln x_{12}\partial_2 - \ln\partial_1 - \ln\partial_2\,. \tag{3.20}$$

In the case of two reggeized gluons we obtain the homogeneous BFKL equation in the form

$$\omega f(\omega,x_1,x_2) = \frac{g^2N}{8\pi^2}\hat{\mathcal{H}}_{GG}f(\omega,x_1,x_2)\,. \tag{3.21}$$

Because of the decomposition (3.20) this equation allows a holomorphically factorized solution.

In the case $r \geq 4$ the gauge group structure of the interaction prevents in general such a factorization. However in the large N approximation this factorization holds. Then the holomorphic part of the r-reggeon equation Fig. 6 corresponds just to the Schrödinger equation of a r-body system in one dimension with the interaction restricted to the nearest neighbours and given by the unconventional hamiltonian $-H_G$ in (3.20). We shall see that it is really an extraordinary hamiltonian.

We use operator relations expressing the derivative operator ∂ as a similarity transformation of x^{-1},

$$\partial = \Gamma(x\partial+1)^{-1}x^{-1}\Gamma(x\partial+1) = \Gamma(-x\partial)x^{-1}\Gamma(-x\partial)^{-1}\,, \tag{3.22}$$

in order to obtain [38]

$$\ln \partial = \tfrac{1}{2}\left(\psi(x\partial) + \psi(1 - x\partial)\right) + (x\partial)^{-1} - \ln x\,. \tag{3.23}$$

The commutation relations between x and ∂ imply

$$\partial^{-1}\ \ln x\ \partial = (x\partial)^{-1}\ \ln x\ (x\partial) = \ln x - (x\partial)^{-1}\,. \tag{3.24}$$

Using (3.23) and (3.24) we obtain

$$H_G = 2\psi(1) - \tfrac{1}{2}\left(\psi(x_{12}\partial_1) + \psi(-x_{12}\partial_2) + \psi(1 - x_{12}\partial_1) + \psi(1 + x_{12}\partial_2)\right)\,. \tag{3.25}$$

$\psi(z)$ is the digamma function,

$$\psi(1) - \psi(z) = \sum_{\ell=0}^{\infty}\left(\frac{1}{\ell + z} - \frac{1}{\ell + 1}\right)\,. \tag{3.26}$$

We neglect the operator $x_{12}(\partial_1 + \partial_2)$ in the following transformation. This is justified in our kinematics, because $i(\partial_1 + \partial_2)$ is the momentum transfer operator and x_{12} is Fourier conjugated to κ. Then (3.25)–(3.26) imply [38]

$$\begin{aligned} H_G &= \chi_0(x_{12}^2\partial_1\partial_2)\,, \\ \chi_\lambda(z) &= \sum_{\ell=0}^{\infty}\left(\frac{2(\ell+\lambda)+1}{(\ell+\lambda)((\ell+\lambda)+1)+z} - \frac{2}{\ell+1}\right)\,. \end{aligned} \tag{3.27}$$

We have obtained H_G as a function of the Casimir operator, $x_{12}^2\partial_1\partial_2$, of holomorphic linear conformal transformations acting on functions of x_1 and x_2. There is another way to show that H_G is conformally invariant. Therefore the result (3.27) holds in general irrespective of the approximation done in the last step.

The symmetry properties hold in the more general case where the (subleading) exchange of reggeized quarks is included. The reggeon interaction in the generalized leading log approximation of QCD is symmetric with repect to linear conformal transformations and allows for holomorphic factorization at large N. After the holomorphic factorization the system of n reggeons can be represented as one-dimensional quantum mechanics of n bodies ordered along a closed (for gluons only) or open (quark and antiquark at the endpoints) string with nearest neighbour interactions.

Infinitesimal conformal transformations of the n reggeon Green function are generated by

$$\begin{aligned} M^a &= \sum_{l=1}^{n} M_\ell^a\,, \\ M_\ell^+ &= x_\ell^2\partial_\ell + 2\Delta_\ell x_\ell\,, \\ M_\ell^- &= \partial_\ell\,, \\ M_\ell^0 &= x_\ell\partial_\ell + \Delta_\ell\,. \end{aligned} \tag{3.28}$$

x_ℓ is the impact parameter and Δ_ℓ the conformal weight of the ℓth reggeon. The anti-holomorphic generators $\tilde{M}^a$ are given by analogous relations with $x_\ell, \partial_\ell, \Delta_\ell$ replaced by $x_\ell^*, \partial_\ell^*, \tilde{\Delta}_\ell$. Reggeized gluons have the conformal weights $\Delta_G = \tilde{\Delta}_G = 0$ and reggeized quarks (depending on helicity , $F, \overline{F}$) have $\Delta_F = 0, \tilde{\Delta}_F = \frac{1}{2}$ and $\Delta_{\overline{F}} = \frac{1}{2}, \tilde{\Delta}_{\overline{F}} = 0$.

All pair interactions of reggeons allow factorization [39]

$$\begin{aligned}
\hat{\mathcal{H}}_{GG} &= H_G + H_G^*\,, \\
\hat{\mathcal{H}}^{(\omega)}_{F\overline{F}} &= H_F^{(\omega)} + P_{12} H_F^{(\omega)*} P_{12}\,, \\
\hat{\mathcal{H}}_{FF} &= H_G + \tilde{H}_F^*\,, \\
\hat{\mathcal{H}}_{FG} &= H_G + P_{12} H_F^{(0)*} P_{12}\,, \\
\hat{\mathcal{G}}_{FG} &= (x_{12}^* \partial_2^*)^{-1} = -P_{12} D_1^{*-1} P_{12}\,.
\end{aligned} \tag{3.29}$$

P_{12} denotes the operator of permutation of x_1 and x_2. We use the notation $D_1 = x_{12}\partial_1$ and $D_2 = x_{12}\partial_2$. The holomorphic parts are functions of the holomorphic Casimir operator,

$$\begin{aligned}
C_{\Delta_1 \Delta_2} &= -M_{12}^{(0)2} + \frac{1}{2}(M_{12}^+ M_{12}^- + M_{12}^- M_{12}^+) \\
&= x_{12}^2 \partial_1 \partial_2 + 2x_{12}(\Delta_1 \partial_2 - \Delta_2 \partial_1) + (\Delta_1 + \Delta_2)(1 - \Delta_1 - \Delta_2)\,.
\end{aligned} \tag{3.30}$$

The holomorphic operators of reggeon interactions are

$$\begin{aligned}
H_G &= \chi_0(C_{00})\,, \\
H_F^{(\omega)} &= \tfrac{1}{2}\left(\chi_{\frac{1-\omega}{2}}\left(C_{0\frac{1}{2}}\right) + \chi_{\frac{\omega-1}{2}}\left(C_{0\frac{1}{2}}\right)\right), \\
\tilde{H}_F &= \chi_0\left(C_{\frac{1}{2}\frac{1}{2}}\right).
\end{aligned} \tag{3.31}$$

and the square of $\mathcal{G}_{FG}$ is the inverse of the antiholomorphic Casimir operator $\tilde{C}_{0\frac{1}{2}}$.

3.4. Complete integrability

We have seen that the system of n reggeons can be viewed as a chain with n sites, where the Hilbert spaces of states at each site ℓ are just representation spaces of $\mathrm{SL}(2,R)$ with weight Δ_ℓ. The case where the Hilbert spaces are representation spaces of $\mathrm{SU}(2)$ and in particular the homogeneous case, where all Δ_ℓ are equal, is well known. For a particular pair interaction the systen is completely integrable and called Heisenberg XXX spin chain.

The $SL(2,R)$ commutation relations obeyed by the generators (3.28) can be expressed in terms of the following r-matrix relation,

$$(L_\ell(\theta_1) \otimes L_\ell(\theta_2))\, R(\theta_1 - \theta_2) = R(\theta_1 - \theta_2)\, (L_\ell(\theta_2) \otimes L_\ell(\theta_1))\ , \qquad (3.32)$$

where $L_\ell(\theta)$ is the following 2×2 matrix

$$L_\ell(\theta) = \begin{pmatrix} \theta + M_\ell^{(0)} & M_\ell^- \\ -M_\ell^+ & \theta - M_\ell^{(0)} \end{pmatrix} . \qquad (3.33)$$

$\otimes$ denotes the tensor product and $R(\theta)$ is a 4×4 matrix with the non-vanishing entries: $R_{11,11}(\theta) = R_{22,22}(\theta) = \theta + 1, R_{12,12}(\theta) = R_{21,21}(\theta) = 1, R_{12,21}(\theta) = R_{21,12}(\theta) = \theta$.

$R(\theta)$ obeys the trilinear Yang-Baxter relation [42]

$$R(\theta_1)R(\theta_2)R(\theta_1 - \theta_2) = R(\theta_1 - \theta_2)R(\theta_2)R(\theta_1) \qquad (3.34)$$

from which one obtains that the operators

$$\tau(\theta) = \mathrm{tr} \prod_{\ell=1}^{n} L_\ell(\theta) \qquad (3.35)$$

with different $\theta_1 \neq \theta_2$ commute. Therefore, $\tau(\theta)$ generates a set of $n-1$ mutually commuting operators.

These operators act non-trivially on all sites $\ell = 1, ..., n$. It is possible to find another set of commuting operators commuting also with $\tau(\theta)$, which are sums of terms, each of which acting only locally, *i.e.* on a few sites ℓ. To this end we consider a second R-matrix relation, involving now $L_\ell(\theta)$ of two sites connected by usual matrix multiplication,

$$(L_1(\theta_1) \cdot L_2(\theta_2))\, \boldsymbol{R}(\theta_1 - \theta_2) = \boldsymbol{R}(\theta_1 - \theta_2)\, (L_2(\theta_2) \cdot L_1(\theta_1))\ . \qquad (3.36)$$

$\boldsymbol{R}$ is an operator acting on functions of x_1 and x_2 and has the property (3.34) of an R-matrix. With $\boldsymbol{R}$ another generator of commuting operators can be constructed in analogy to (3.35), where the multiplication and the trace are defined in the space of functions of x. The first operator appearing in the θ expansion is a sum of operators acting on two neighbouring sites. It is natural to view it as the hamiltonian of the system. It can be obtained by expanding $\boldsymbol{R}(\theta)$.

$$\boldsymbol{R}(\theta) = P_{12}\left(1 - \theta H_G + \mathcal{O}(\theta^2)\right)\ . \qquad (3.37)$$

From this expansion and (3.36) one can easily calculate this operator and check that it is just the operator of reggeized gluon interaction (3.27).

We have outlined the way how one establishes the complete integrability of the reggeon interaction in QCD. Unfortunately the standard procedure for deriving the eigenstates and eigenvalues, the algebraic Bethe ansatz, does not work here. An approach based on the functional Bethe ansatz has been proposed and shown to reproduce the known result in the case of the two-gluon exchange. More details are given in the talk by G. Korchemsky.

4. Applications of the perturbative pomeron

4.1. The BFKL pomeron

In our notations the BFKL pomeron is represented by the Green function $f(\omega, x_1, x_2; \bar{x}_1, \bar{x}_2)$ of two reggeized gluons in the leading log approximation, which is the solution of the equation

$$\omega f = f^{(0)} + \frac{g^2 N}{8\pi^2} \mathcal{H}_{GG} f\,,$$
$$|\partial_1|^2 |\partial_2|^2 f^{(0)}(\omega, x_1, x_2; \bar{x}_1, \bar{x}_2) = \delta(x_1 - \bar{x}_1)\delta(x_2 - \bar{x}_2)\,. \qquad (4.1)$$

The solution is now straightforward after having understood the properties of conformal symmetry and factorizability of $\mathcal{H}_{GG}$ and using its representation (3.27) in terms of conformal Casimir operators.

Eigenfunctions of the homogeneous equation are the conformal 3-point functions,

$$\begin{aligned} E(x_{10}, x_{20}) &= \left\langle \phi^{(\Delta_1, \tilde{\Delta}_1)}(x_1) \phi^{(\Delta_1, \tilde{\Delta}_1)}(x_2) \mathcal{O}^{(m, \tilde{m})}(x_0) \right\rangle \\ &= \left(\frac{x_{12}}{x_{10} x_{20}} \right)^{m - \Delta_1 - \Delta_2} x_{10}^{-2\Delta_1} x_{20}^{-2\Delta_2} \\ &\quad \cdot \left(\frac{x_{12}^*}{x_{10}^* x_{20}^*} \right)^{\tilde{m} - \tilde{\Delta}_1 - \tilde{\Delta}_2} x_{10}^{*-2\tilde{\Delta}_1} x_{20}^{*-2\tilde{\Delta}_2}\,. \end{aligned} \qquad (4.2)$$

They form a twofold overcomplete set of functions of two impact parameters x_1, x_2, which transform under the linear conformal group generated by $M_1^a(\Delta_1) + M_2^a(\Delta_2), \tilde{M}_1^a(\tilde{\Delta}_1) + \tilde{M}_2^a(\tilde{\Delta}_2)$ (3.28). In the unitary series of representations the conformal weights of the two-reggeon state $m, \tilde{m}$ are given by

$$m = \frac{1}{2} + i\nu + \frac{n}{2}\,, \qquad \tilde{m} = \frac{1}{2} + i\nu - \frac{n}{2}\,, \qquad (4.3)$$

where n takes all integer and ν takes all real values. The eigenvalues of the holomorphic and antiholomarphic Casimir operators are $m(1-m)$ and

$\tilde{m}(1-\tilde{m})$, respectively. The impact parameter x_0 labels the states the states within one representation.

Thus the eigenfunctions are given by (4.2) for the gluon case, $\Delta_1 = \Delta_2 = 0, \tilde{\Delta}_1 = \tilde{\Delta}_2 = 0$. From (3.27) we have for the eigenvalues

$$\begin{aligned} \mathcal{H}_{GG} E^{(n,\nu)} &= \Omega_{GG}(n,\nu) E^{(n,\nu)}, \\ \Omega_{GG}(n,\nu) &= \chi_0(m(1-m)) + \chi_0(\tilde{m}(1-\tilde{m})). \end{aligned} \tag{4.4}$$

For $\chi_0(m(1-m))$ we have the following expression in terms of $\psi(z)$,

$$\chi_0(m(1-m)) = 2\psi(1) - \psi(m) - \psi(1-m). \tag{4.5}$$

We use the completeness relation of the eigenfunctions (4.2),

$$\delta(x_1 - \overline{x}_1)\delta(x_2 - \overline{x}_2) = \int_{-\infty}^{\infty} d\nu \sum_{n=-\infty}^{\infty} G_{n,\nu} \frac{E^{(n,\nu)*}(x_{10}, x_{20}) E^{(n,\nu)}(\overline{x}_{10}, \overline{x}_{20})}{|x_{12}|^2 |\overline{x}_{12}|^2},$$

$$G_{n,\nu} = 16(\nu^2 + \frac{n^2}{4}), \overline{x}_{10} = \overline{x}_1 - x_0, \tag{4.6}$$

to obtain the solution of the inhomogeneous equation (4.1), [36]

$$f(\omega, x_1, x_2; \overline{x}_1, \overline{x}_2) = \int_{-\infty}^{\infty} d\nu \sum_{n=-\infty}^{\infty} G_{n,\nu} B_{n,\nu}^{-1} \frac{E^{(n,\nu)*}(x_{10}, x_{20}) E^{(n,\nu)}(\overline{x}_{10}, \overline{x}_{20})}{\omega - \frac{g^2 N}{8\pi^2} \Omega(n,\nu)},$$

$$B_{n,\nu} = \frac{1}{16} G_{n-1,\nu} G_{n+1,\nu}. \tag{4.7}$$

This is the Green function of the BFKL pomeron. The singularities in ω emerge from pinching of the ν-integration path by poles at $\pm i\nu(n,\omega)$ at the positions

$$\omega_n = \frac{g^2 N}{8\pi^2} \Omega_{GG}(n,0). \tag{4.8}$$

They are square-root branch points. The leading singularity is the one for conformal spin $n = 0$. We use (4.5) and $\psi(\frac{1}{2}) = \psi(1) - 2\ln 2$.

$$\omega_0 = \frac{g^2 N}{8pi^2} \Omega_{GG}(0,0) = \frac{g^2 N}{2\pi^2} 2\ln 2. \tag{4.9}$$

We have reproduced the well known result [2], which we have used already in (1.7).

The eigenvalues can be obtained more easily in the momentum representation, if one restricts to the particular case of vanishing momentum

transfer, $q = 0$. In this case the eigenfunctions $E^{(n,\nu)}$ are replaced by the following complete set of eigenfunctions,

$$E^{(n,\nu)} \to \varphi_{n,\nu}(\kappa) = |\kappa^2|^{1/2+i\nu} \left(\frac{\kappa^*}{|\kappa|}\right)^n , \tag{4.10}$$

and the pomeron Green function is given by

$$\tilde{f}(\omega, \kappa, \bar{\kappa}, 0) = \frac{1}{2\pi^2} \int_{-\infty}^{\infty} d\nu \sum_{n=-\infty}^{\infty} \frac{|\kappa^2|^{1/2+i\nu} \left(\frac{\kappa}{|\kappa|}\right)^n |\bar{\kappa}^2|^{1/2-i\nu} \left(\frac{\bar{\kappa}}{|\bar{\kappa}|}\right)^{-n}}{\omega - \frac{g^2 N}{8\pi^2} \Omega(n,\nu)} . \tag{4.11}$$

We recall that κ is the Fourier conjugate to $x_{12} = x_1 - x_2$ and q is conjugate to $R = (x_1 + x_2)/2$.

Sometimes the mixed representation is useful, with the variables q and $\rho = x_{12}$,

$$E^{(n,\nu)}(\rho, q) = \int e^{iRq} E^{(n,\nu)}(R - \frac{\rho}{2}, R + \frac{\rho}{2}) . \tag{4.12}$$

In this representation the 3-point fuctions have a simple asymptotics at $\rho q \ll 1$,

$$E^{(n,\nu)}(\rho, q) \sim r_{n,\nu} \left(|\rho|^{-2i\nu} + |q^2 \rho|^{2i\nu} e^{i\delta(n,\nu}\right) . \tag{4.13}$$

$r_{n,\nu}$ and $\delta(n,\nu)$ are known.

This asymptotics has been used to calculate the coefficients in the completeness and orthogonality relations [37]. The two-reggeon Green function in the mixed representation is given by

$$\tilde{f}(\omega, \rho, \bar{\rho}, q) = \int_{-\infty}^{\infty} d\nu \sum_{n=-\infty}^{\infty} B^{-1}_{n,\nu} \frac{E^{(n,\nu)*}(\rho, q) E^{(n,\nu)}(\bar{\rho}, q)}{\omega - \frac{g^2 N}{8\pi^2} \Omega(n,\nu)} . \tag{4.14}$$

4.2. Renormalization group and pomeron poles

The above results concern an approximation to perturbative QCD which is a good approximation in the perturbative Regge region. In particular conformal symmetry (and related to this the Regge singularities appearing as fixed branch points) holds only in this approximation. In general conformal symmetry is broken by renormalization.

We recall that in the range of applicability of this approximation all transverse momenta are of the same order $|q|$ and that this scale obeys $s \gg |q|^2 \gg m_p^2$.

In the following discussion it is convenient from the general case of non-vanishing momentum transfer, $|q|^2 = |\kappa_1 - \kappa_2|^2 \sim |\kappa_1|^2 \sim |\kappa_2|^2 \sim |\kappa_1'|^2 \sim |\kappa_2'|^2$. The result for the Regge singularities does not change in the particular case of vanishing momentum transfer.

In deep-inelastic scattering we encounter the situation

$$Q^2 \geq |\kappa|^2 \gg |\kappa'|^2 \sim |q|^2 , \tag{4.15}$$

where $\kappa = (\kappa_1 + \kappa_2)/2$. The perturbative Regge result (leading $\ln x$ appreoximation) is still applicable if the logarithm of the transverse momentum ratio is not too large,

$$\alpha_S(\kappa') \ln |\frac{\kappa}{\kappa'}|^2 \ll 1 . \tag{4.16}$$

The large κ behaviour of $f_{2\to 2}(\omega, \kappa, \kappa', q)$ is described by the GLAP equation [10], which is based on the renormalization group. In an intermediate range, where the logarithm of the transverse momentum ratio is still not too large, the perturbative Regge result ($\ln x$ approximation) and the renormalization group ($\ln \kappa^2$ approximation) have to match approximately. This matching condition restricts in particular the allowed scaling dimensions ν compared to the perturbative Regge result, where ν takes all real values (4.14). The integral over ν reduces to a discrete sum and as a consequence the branch cuts in ω convert into series of poles. This is the way how the breaking of conformal symmetry by renormalization affects the Regge singularities [36, 37].

The effect of scale breaking can be incorporated also by modifying the BFKL equation by infrared and ultraviolet cut-offs in the transverse momenta [50].

To reproduce the result for the pomeron poles in some detail we start with the representation (4.14) of the BFKL Green function, restrict to the leading term $n = 0$ and do the ν integral by taking the residue in one of the two poles

$$\overline{\nu}(\omega, \frac{g^2}{4\pi}) = \pm \left(\frac{14\pi^2 \zeta(3)}{g^2 N} \right)^{1/2} \sqrt{\omega_0 - \omega} , \tag{4.17}$$

where ω_0 is given in (4.9). We obtain the approximate perturbative Regge solution,

$$f_R(\omega, \rho, \overline{\rho}, q) \approx E^{(\overline{\nu}(\omega))*}(\rho, q) E^{(\overline{\nu}(\omega))}(\overline{\rho}, q) . \tag{4.18}$$

The large κ asymptotics corresponds to the small ρ asymptotics in this representation. The latter asymptotics is given by (4.13) applied to the first factor in (4.18). We have two terms $f_{R\pm}$ with scaling dimensions differing in sign,

$$i|\rho|^2 \frac{\partial}{\partial |\rho|^2} f_{R\pm}(\omega, \rho) = \pm \overline{\nu}\left(\omega, \frac{g^2}{4\pi}\right) f_{R\pm}(\omega, \rho) . \tag{4.19}$$

We encounter the standard situation in the renormalization group analysis. To become compatible with the renormalization group we have to replace the coupling by the running coupling,

$$\overline{\nu}\left(\omega, \frac{g^2}{4\pi}\right) \to \overline{\nu}(\omega, \alpha_S(|\rho|^{-2}))$$

$$\alpha_S\left(\frac{1}{|\rho|^2}\right) = \frac{-b}{\ln(|\rho|^2\Lambda^2)}, \quad \frac{4\pi}{b} = 11 - \frac{2}{3}N_f\,. \tag{4.20}$$

This corresponds to summing the leading logarithms in the ratio of the transverse momenta.

For our purpose it is more convenient to rewrite the scaling relation (4.19) in the following form close to the eigenvalue equation,

$$\omega - \frac{g^2 N}{8\pi^2}\Omega(0,\nu) = 0\,, \tag{4.21}$$

the solutions of which are $\pm\overline{\nu}\left(\omega, \frac{g^2}{4\pi}\right)$,

$$\left(\omega - \frac{g^2 N}{8\pi^2}\Omega\left(0, i\frac{\partial}{\partial \ln|\rho|^2}\right)\right) f_R(\rho) = 0\,. \tag{4.22}$$

This form is valid for both scaling terms $f_{R\pm}$,

$$f_R(\rho) \sim |\rho|^{2i\overline{\nu}(\omega,\frac{g^2}{4\pi})} + |q^2\rho|^{-2i\overline{\nu}(\omega,\frac{g^2}{4\pi})} e^{\delta(\overline{\nu}(\omega,\frac{g^2}{4\pi}))}\,. \tag{4.23}$$

According to (4.20) the modified scaling relation compatible with the renormalization group can be written as

$$\left(\omega - \frac{N}{2\pi}\alpha_S(|\rho|^{-2})\Omega\left(0, i\frac{\partial}{\partial \ln|\rho|^2}\right)\right) f_{DI}(\rho) = 0\,. \tag{4.24}$$

The solution is given by the integral

$$f(\rho) = \int_{-\infty}^{\infty} d\nu \exp\left[-i\nu\ln(|\rho|^2\Lambda^2) + \frac{ibN}{2\pi\omega}\int_0^{\nu}\Omega(\nu', n)d\nu'\right]\,. \tag{4.25}$$

The behaviour for small ρ, where the modified scaling relation is to be applied, is given by the saddle point approximation of this integral. The

saddle point is at $\overline{\nu}(\omega, \alpha_S(|\rho|^{-2}))$. At not too small ρ, where ω_0 is still larger then ω, we have

$$f_{DI}(\rho) \sim \cos\left(\frac{\pi}{4} - \overline{\nu}(\omega, \alpha_S(|\rho|^{-2}))\ln(|\rho|^2\Lambda^2) - \frac{Nb}{2\pi\omega}\int_0^{\overline{\nu}(\omega,\alpha_S)} d\nu' \Omega(0,\nu')\right). \tag{4.26}$$

The condition of continuity of the logarithmic derivatives of both solutions at $\rho \sim \overline{\rho} \sim q^{-1}$ can be written by using the approximations for $\Omega(0,\nu)$ and $\delta(\nu)$ at small ν,

$$\tfrac{1}{4}\Omega(0,\nu) = 2\ln 2 - 7\zeta(3)\nu^2 + \mathcal{O}(\nu^4), \delta(\nu) = \pi + \mathcal{O}(\nu). \tag{4.27}$$

We obtain the following restriction on the allowed scaling dimensions ν (r is integer),

$$\nu_r = \left(\frac{3\pi\ln 2(r+3/2)}{7\zeta(3)\ln\frac{q^2}{\Lambda^2}}\right)^{1/3}. \tag{4.28}$$

In the solution (4.7) for the pomeron Green function the integral over ν has to be replaced by a sum over ν_r and therefore we obtain the pomeron poles

$$\omega_r(q) = \frac{4N}{\pi}\ln 2\alpha_S(q)\left(1 - \left(\ln\frac{q^2}{\Lambda^2}\right)^{-2/3}\left(\frac{7\zeta(3)}{2\ln 2}\right)^{1/3}(r+3/4)^{2/3}\right). \tag{4.29}$$

This holds for $\kappa > \overline{\kappa} \sim q$. For the particular case of vanishing momentum transfer the scale q is to be replaced by $\overline{\kappa}$, the smaller of the external momenta of the reggeon Green function.

By this continuity argument we find the scale of the coupling in the BFKL intercept and a correction. Estimating the leading ($r = 0$) pole position by substituting for α_S the value resulting in the usually quoted $\alpha_{BFKL} - 1 = 0.5$ we obtain that the correction factor in (4.29) reduces this value by (1- 0.3). We notice also that due to the correction factor the scale dependence of the result (4.29) is less than that of the first factor.

4.3. The $2 \to 4$ reggeon vertex

We describe the construction [43] of the $2 \to 4$ reggeon vertex in the generalized leading log approximation. This vertex enters as a building block the perturbative contribution to diffractive amplitudes. It determines the weight of the 4-reggeon correction to the structure function at small x, because the virtual photon couples via a quark loop dominantly to 2 gluons.

The construction is non-trivial mainly due to the bootstrap property discussed in Section 3.1. First one constructs the particle-reggeon vertices D_n (1.23) for $n = 2, 3, 4$ reggeons. Then the reducible contributions $D_{n,r}$, which are not true 4-reggeon states, have to be removed. Finally the result is factorized,

$$\left(D_4^{(R+)} - D_{4,r}^{(R+)}\right) = D_2 \otimes V_{2\to 4}^{(R)} \otimes f_{4\to 4}^{(R+)}\,, \tag{4.30}$$

in order to extract the vertex $V_{2\to 4}^{(R)}$.

The four reggeized gluons are in the overall gauge group singlet and signature even state. To specify further this state we use the basis with a definite signature $\sigma = \pm$ and the gauge group representation R of the pair (34) of the reggeons $\ell = 1, 2, 3, 4$. In the case of SU(3) the tensor product of two adjoint representations decomposes into the singlet O, the antisymmetric A and the symmetric V octets, two decuplets Δ, conjugate to each other, and the symmetric 27 dimensional representation S. We are going to explain some details for the subchannel with the pairs (12) and (34) in the positive signature singlet state $(O+)$.

In the leading log approximation we have

$$D_2 = \Phi_2 \otimes f_{2\to 2}\,, \tag{4.31}$$

where $f_{2\to 2}$ is the solution of the BFKL equation (4.11). $\Phi_2(\kappa_1, \kappa_2)$ is the impact factor [20] coupling 2 reggeized gluons to the external (in- and outgoing) virtual photon *via* a quark loop. $\otimes$ denotes the integration over the gluon transverse momenta κ_1, κ_2 with the momentum transfer $q = \kappa_1 + \kappa_2$ fixed.

The state of three exchanged gluons in the overall signature even singlet state is specified *e.g.* by the signature $\sigma = \pm$ of the pair (23).

$$D_3^{(\sigma)} = (\Phi_3^{(\sigma)} + D_2 \otimes K_{2\to 3}^{(\sigma)}) \otimes f_{3\to 3}^{(\sigma)}\,. \tag{4.32}$$

$f_{3\to 3}^{(\sigma)}$ is the solution of (3.13) for $n = 3$. The 3-reggeon impact factor of the virtual photon reduces to the 2-reggeon impact factor,

$$\begin{aligned}
\Phi_3^{(-)}(\kappa_1, \kappa_2, \kappa_3) &= g\frac{\sqrt{3}}{2}\Phi_2(\kappa_1, \kappa_2 + \kappa_3)\,, \\
\Phi_3^{(+)}(\kappa_1, \kappa_2, \kappa_3) &= g\frac{\sqrt{3}}{2}(\Phi_2(\kappa_1 + \kappa_2, \kappa_3) - \Phi_2(\kappa_1 + \kappa_3, \kappa_2))\,.
\end{aligned} \tag{4.33}$$

Similar to the two-reggeon interaction kernel (3.12) the transition kernel $K_{2\to 3}$ can be obtained both from the transverse momentum parts of the

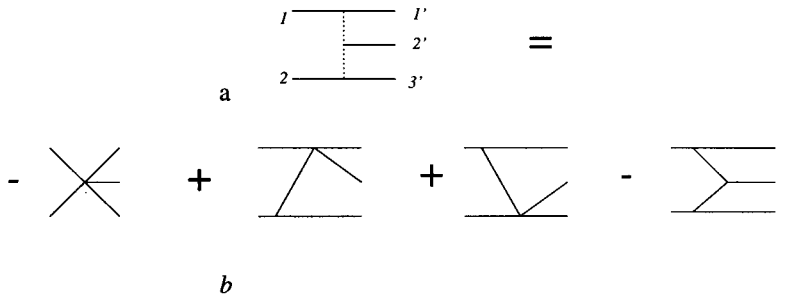

Fig. 8. The transition kernel $2 \to 3$ in s-channel — a, and t-channel — b representation.

vertices $\mathcal{L}_p$ and $\mathcal{L}_t$, Fig. 8. In the latter case higher vertices have to be introduced which can be understood as emerging from graphs with triple only vertices by contracting lines, the propagator of which are cancelled by factors in the adjacent vertices.

$$K_{2\to 3}(\kappa_1,\kappa_2;\kappa_1',\kappa_2',\kappa_3') = \frac{\kappa_1\kappa_1'^*\kappa_2^*\kappa_3'}{(\kappa_1-\kappa_1')^*(\kappa_2-\kappa_3')} + \text{c.c.}$$

$$= -|\kappa_1+\kappa_2|^2 + \frac{|\kappa_1'+\kappa_2'|^2|\kappa_2|^2}{|\kappa_2-\kappa_3'|^2}$$

$$+ \frac{|\kappa_2'+\kappa_3'|^2|\kappa_1|^2}{|\kappa_1-\kappa_1'|^2} - \frac{|\kappa_1|^2|\kappa_2|^2|\kappa_2'|^2}{|\kappa_2-\kappa_3'|^2|\kappa_1-\kappa_1'|^2}\,. \tag{4.34}$$

The projection $K_{2\to 3}^{(\sigma)}$ is obtained from this expression by symmetrizing or antisymmetrizing in the momenta (23) similar to (4.33). Due to the bootstrap property D_3 can be expressed in terms of D_2 by the relations (4.33) with Φ_2 replaced by D_2.

Now the particle 4-reggeon vertex is constructed as

$$D_4^{(R,\sigma)} = (\Phi_4^{(R,\sigma)} + D_2 \otimes K_{2\to 4}^{(R,\sigma)} + \{D_3 \otimes K_{2\to 3}\}^{(R,\sigma)}) \otimes f_{4\to 4}^{(R,\sigma)}\,. \tag{4.35}$$

Also the 4-gluon impact factor of the virtual photon reduces in the leading log approximation to the 2-gluon impact factor. For the subchannel $(O,+)$ one finds

$$\Phi_4^{(O+)}(\kappa_1,\kappa_2,\kappa_3,\kappa_4) = -\frac{g^2\sqrt{2}}{3}[(\Phi_2(\kappa_1,\kappa_2+\kappa_3+\kappa_4) + \text{cycl.perm. of } \kappa_1,\kappa_2,\kappa_3,\kappa_4) - (\Phi_2(\kappa_1+\kappa_2,\kappa_3+\kappa_4) + \text{cycl.perm. of } \kappa_2,\kappa_3,\kappa_4)]. \tag{4.36}$$

The transition kernel $K_{2\to4}$ can be obtained in analogy to $K_{2\to3}$, Fig. 9,

$$\begin{aligned} K_{2\to4}(\kappa_1,\kappa_2;\kappa_1',\kappa_2',\kappa_3',\kappa_4') &= \frac{\kappa_1\kappa_1'^*\kappa_2^*\kappa_4'}{(\kappa_1-\kappa_1')^*(\kappa_2-\kappa_4')} + \text{c.c.} \\ &= -|\kappa_1+\kappa_2|^2 + \frac{|\kappa_1'+\kappa_2'+\kappa_3'|^2|\kappa_2|^2}{|\kappa_2-\kappa_4'|^2} \\ &\quad + \frac{|\kappa_2'+\kappa_3'+\kappa_4'|^2|\kappa_1|^2}{|\kappa_1-\kappa_1'|^2} \\ &\quad - \frac{|\kappa_1|^2|\kappa_2|^2|\kappa_2'+\kappa_3'|^2}{|\kappa_2-\kappa_4'|^2|\kappa_1-\kappa_1'|^2}. \end{aligned} \tag{4.37}$$

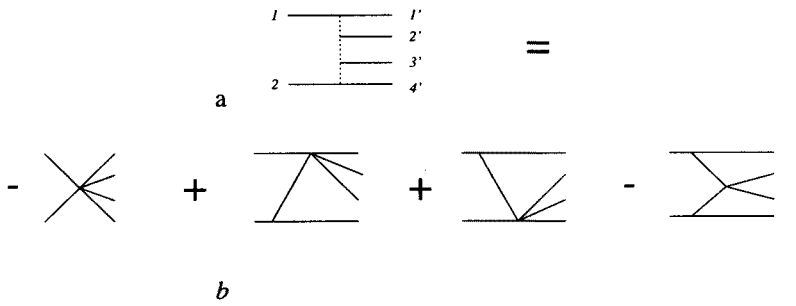

Fig. 9. The transition kernel $2 \to 4$ in s-channel — a, and t-channel — b transitions.

The projections $K_{2\to4}^{(R;\sigma)}$ are obtained by (anti)symmetrizations and by multiplication with group factors. The third term in (4.35) are the contributions from transitions of a pair out of 3 reggeons into 3 with the projection to the 4-reggeon subchannel (R,σ).

The contributions of the signature odd octet states $(A,-)$ in the pairs (13), (24) or (14), (23) has to be eliminated, because they reduce to a 2-reggeon state. For the subchannel $(O,+)$ this reducible part $D_{4,r}^{(O+)}$ is given by the analogous expression (4.36) with Φ_2 replaced by D_2.

According to [43] the result for the vertex can be expressed in terms of a modified two-reggeon interaction kernel (3.18)

$$\tilde{\mathcal{H}}_{GG}(\kappa_1,\kappa_2,\kappa_1',\kappa_2') = \mathcal{H}_{GG}(\kappa_1,\kappa_2,\kappa_1',\kappa_2') + \alpha_G(\kappa_1+\kappa_2)(\delta(\kappa_1-\kappa_1')\delta(\kappa_2-\kappa_2'))\,. \quad (4.38)$$

$$V^{a_1a_2a_3a_4}((\kappa_1,\kappa_2,\kappa_1',\kappa_2') = \frac{g^2}{12\sqrt{2}}\{\delta^{a_1a_2}\delta^{a_3a_4}[\tilde{\mathcal{H}}_{GG}(\kappa_1,\kappa_2;\kappa_1',\kappa_3') + \tilde{\mathcal{H}}_{GG}(\kappa_1,\kappa_2;\kappa_2',\kappa_3') + \tilde{\mathcal{H}}_{GG}(\kappa_1,\kappa_2;\kappa_1',\kappa_4') + \tilde{\mathcal{H}}_{GG}(\kappa_1,\kappa_2;\kappa_2',\kappa_4') - \tilde{\mathcal{H}}_{GG}(\kappa_1,\kappa_2;\kappa_1',\kappa_3'+\kappa_4') - \tilde{\mathcal{H}}_{GG}(\kappa_1,\kappa_2;\kappa_2',\kappa_3'+\kappa_4') - \tilde{\mathcal{H}}_{GG}(\kappa_1,\kappa_2;\kappa_1'+\kappa_2',\kappa_3') - \tilde{\mathcal{H}}_{GG}(\kappa_1,\kappa_2;\kappa_1'+\kappa_2',\kappa_4') + \tilde{\mathcal{H}}_{GG}(\kappa_1,\kappa_2;\kappa_1'+\kappa_2',\kappa_3'+\kappa_4')] + (2\leftrightarrow 3) + (2\leftrightarrow 4)\}\,. \quad (4.39)$$

4.4. Amplitudes for the hadronic final states

Data about the hadronic final states in deep-inelastic scattering provide tests of the interaction mechanism in particular at small x. Consider the one-jet inclusive distribution, *i.e.* fix a jet with κ_j, x_j and sum over all other produced hadrons. As pointed out by Mueller [9] the most interesting configuration at small x is the case where $x \ll x_j$ but $|\kappa_j|^2 \sim Q^2$. This selects a parton evolution starting from the radiation of the parton j producing this jet up to the quark struck by the virtual photon, which goes essentially in the y direction. In this case the Kancheli–Mueller amplitude describing this inclusive distribution has the form

$$\Phi_2^\gamma \otimes f_{2\to 2} \otimes \Phi_M\,. \quad (4.40)$$

The impact factor Φ_M describes the coupling of the 2 reggeized gluons to the in forward direction in- and outgoing parton (which is dominantly a gluon g) and to the proton, Fig.10. According to [44] it can be substituted by the convolution of the parton distribution $q_{i/p}(x_i,|\kappa_j|^2)$ with the parton splitting kernel $i \to gi$ with a sum over the parton type i.

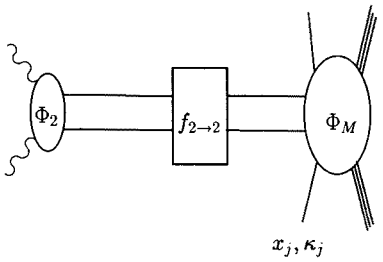

Fig. 10. One-gluon (jet) inclusive distribution.

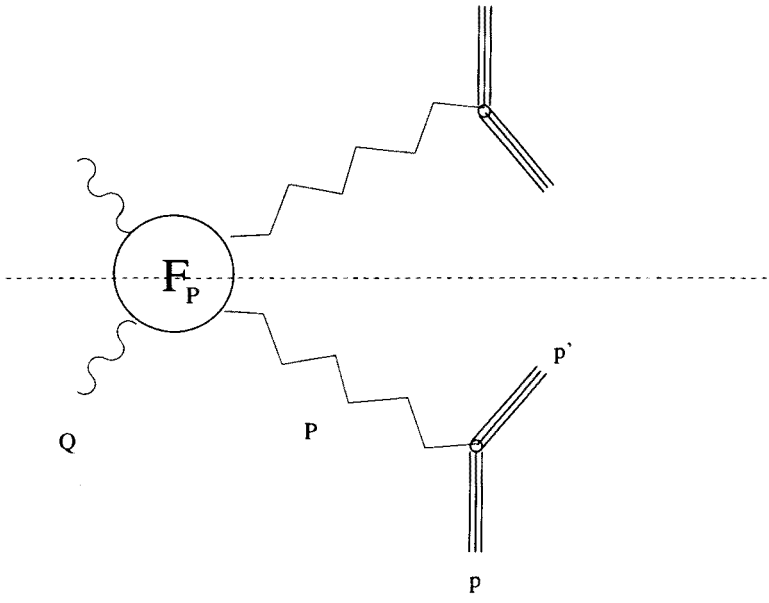

Fig. 11. Proton diffraction.

The preliminary data [5] on jet rates in this kinematics seem to be compatible with the expectations of (4.40) and by a factor 2 higher than models simulating the r-evolution.

The inclusive amplitude (4.40) can be used to calculate the transverse energy flow at small x. It has been shown [45] that the energy flow expected by the perturbative Regge calculations is significantly higher compared to the predictions of "conventional" r-evolution (parton shower) models. The data confirm the perturbative Regge predictions.

Rapidity gap events originating from proton diffraction have attracted much attention [47]. The diffractive cross section is given by the Kancheli–Mueller graph, Fig. 11, and has the form

$$F_P(\frac{x}{x_P}, Q^2) \otimes \left(f_P(x_P) \otimes \Phi_{pp'}\right)^2 . \tag{4.41}$$

p' is the momentum of the scattered (low-mass excitation of the) proton and $\beta = \frac{x}{x_P} = \frac{Q^2}{2(p-p')(k_e-k'_e)}$. The latter can be considered as the Bjorken variable of the deep-inelastic scattering off the pomeron P and then F_P is considered as the pomeron structure function [46]. Because there is not necesserily a large transverse momentum in the pomeron Green function f_P it cannot be replaced by the perturbative BFKL Green function $F_{2\to 2}$. The

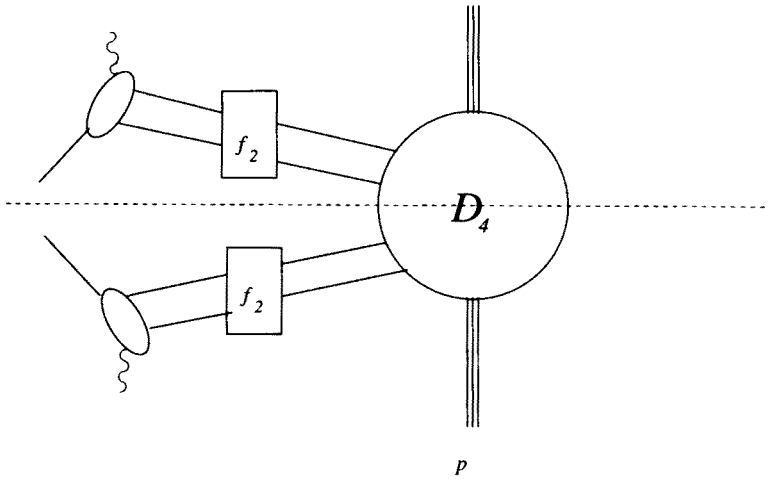

Fig. 12. $\gamma^* p$ diffraction.

analysis of the data shows that the x_P dependence (at fixed β) follows the "soft" pomeron intercept of the hadron phenomenology.

The perturbative contribution to this process has been calculated [43]. It involves the $2 \to 4$ reggeon vertex discussed above. Additional kinematic restrictions, *e.g.* relatively large $t = (p - p')^2$, have to be imposed in order to enhance the perturbative contribution.

In the deep-inelastic diffractive process $\gamma^* p \to VX$, where V is a vector meson, the perturbative contribution dominates without additional conditions. The corresponding Kancheli–Mueller amplitude has the structure (Fig. 12)

$$\left(\Phi_{\gamma^* V} \otimes f_{2\to 2}\right)^2 \otimes D_{4/p}^{(O+)}, \tag{4.42}$$

where $D_{4/p}$ stands for the vertex function coupling 4 reggeized gluons to the scattering proton. If Q^2 or the $\gamma^* V$ momentum transfer are large compared to m_p^2 or if V consists of heavy quarks then the perturbative calculations apply [48]. The preliminary data [5] show that indeed the x dependence is of BFKL type.

The author is grateful to the organizers of this interesting school for invitation. He likes to thank R. Engel, L.N. Lipatov, L. Szymanowski and A. White for useful discussions.

REFERENCES

[1] A. Donnachie, P.V. Landshoff, *Nucl. Phys.* **B244**, 322 (1984); *Phys. Lett.* **B296**, 227 (1992).

[2] V.S. Fadin, E.A. Kuraev, L.N. Lipatov, *Phys. Lett.* **60B**, 50 (1975); *Zh. Exp. Teor. Fiz.* **71**, 840 (1976); *Zh. Eksp. Teor. Fiz.* **72**, 377 (1977); Y.Y. Balitski, L.N. Lipatov, *Sov. J. Nucl. Phys.* **28**, 882 (1978).

[3] I. Abt *et al.*, H1 Collab., *Nucl. Phys.* **B407**, 515 (1993).

[4] M. Derrick *et al.*, Zeus Collab., *Phys. Lett.* **316B**, 412 (1993).

[5] A. de Roeck, Physics results from HERA, preprint DESY 95-025 (1995).

[6] V.N. Gribov, L.N. Lipatov, *Sov. J. Nucl. Phys.* **15**, 78 (1971).

[7] Yu.L. Dokshitzer, D. Dyakonov, S.I. Troyan, *Phys. Rep.* **58**, 270 (1980).

[8] B.I. Ermolaev, V.S. Fadin, *Pisma Zh. Eksp. Teor. Fiz.* **33**, 285 (1981); Yu.L. Dokshitzer, V.S. Fadin, V.A. Khoze, *Phys. Lett.* **115B**, 245 (1982); Ya.I. Azimov, Yu.L. Dokshitzer, V.A Khoze, S.I. Troyan, *Z. Phys.* **C27**, 65 (1985); and **C31**, 231 (1986).

[9] A.H. Mueller, H. Navelet, *Nucl. Phys.* **B282**, 727 (1987); A.H. Mueller, *Nucl. Phys. B (Proc. Suppl)* **18C**, 125 (1991); A.H. Mueller and W.-K. Tang, *Phys. Lett.* **284B** (1992) 123; V. del Duca, An introduction to the pert. QCD pomeron and to jet physics at large rapidities, preprint DESY 95-023.

[10] V.N. Gribov, L.N. Lipatov, *Sov. J. Nucl. Phys.* **15**, 78 (1971); L.N. Lipatov, *Sov. J. Nucl. Phys.* **20** ,94 (1974); Yu.L. Dokshitzer, *Sov. Phys. JETP* **46**, 641 (1977); G. Altarelli, G. Parisi, *Nucl. Phys.* **B126**, 289 (1977).

[11] J. Collins, R.K. Ellis, *Nucl. Phys.* **B360**, 3 (1991); J.R. Forshaw, R.G. Roberts, Rutherford preprint RAL 94-028; J. Blümlein, DESY preprint 94/149; J. Kwieciński, A.D. Martin, Durham preprint DTP/95/34.

[12] H. Cheng, C.Y. Lo, *Phys. Rev.* **D13**, 1131 (1976); *Phys. Rev.* **D15**, 2959 (1977).

[13] L.V. Gribov, E.M. Levin, M.G. Ryskin, *Phys. Rep.* **100C**, 1 (1983).

[14] A.H. Mueller, *Nucl. Phys.* **B415**, 377 (1994); N.N. Nikolaev, B.G. Zakharov, *Phys. Lett.* **B327**, 149, 157 (1994); **B328**, 486 (1994); **B333**, 806 (1994).

[15] M. Ciafaloni, *Nucl. Phys.* **B296**, 99 (1988); S. Catani, F. Fiorani, G. Marchesini; *Phys. Lett.* **B234**, 339 (1990); *Nucl. Phys.* **B336**, 18 (1990); G. Marchesini, in Proceedings of *QCD at 200TeV*, Erice, June 1990, ed. by L. Ciafarelli and Yu.L. Dokshitzer, Plenum Press, NY 1992, p. 183; Milano preprint IFUM-486-FT (Nov. 1994)

[16] A.D. Martin, R.G. Roberts, W.J. Stirling, *Phys. Lett.* **306B**, 145 (1993).

[17] M. Glück, E. Reya, A. Vogt, *Phys. Lett.* **306B**, 391 (1993).

[18] R.D. Ball, S. Forte, *Phys. Lett.* **B335**, 77 (1994); **B336**, 77 (1994); CERN preprints TH 7421/94 and 7422/94.

[19] S. Catani, M. Ciafaloni, F. Hautmann, *Phys. Lett.* **B242**, 97 (1990); *Nucl. Phys.* **B366**, 657 (1991); S. Catani, F. Hautmann, *Nucl Phys.* **B472**, 475 (1994).

[20] H. Cheng, T.T. Wu, *Expanding Protons: Scattering at High Energies*, The MIT Press, 1987; B.M. McCoy, T.T. Wu, *Phys. Rev.* **D12**, 3257 (1975) and

D13,1076 (1976); H. Cheng, C.Y. Lo, *Phys. Rev.* **D13**,1131 (1976) and **D15**, 2959 (1977).

[21] V.G. Gorshkov, V.N. Gribov, L.N. Lipatov, G.V. Frolov, *Yad. Fiz.* **6**, 129 and 361 (1967); V.N. Gribov, L.N. Lipatov, G.V. Frolov, *Sov. J. Nucl. Phys.* **12**, 543 (1971).

[22] J. Bartels, *Nucl. Phys.* **B151**, 293 (1979); *Nucl. Phys.* **B175**, 365 (1980).

[23] J. Kwieciński, M. Praszalowicz, *Phys. Lett.* **B94**, 413 (1980).

[24] A.R. White, *Int. J. Mod. Phys.* **A6**, 1859 (1990).

[25] L.N. Lipatov in *Perturbative QCD*, A.H. Mueller ed., World Scientific, Singapore 1989.

[26] L.N. Lipatov, *Nucl. Phys.* **B365**, 614 (1991).

[27] R. Kirschner, L.N. Lipatov, L. Szymanowski, *Nucl. Phys.* **B425**, 579 (1994); *Phys. Rev.* **D51**, 838 (1995).

[28] R. Kirschner, L. Szymanowski, Trieste preprint SISSA Ref. 194/94/EP 1994, to be published in *Phys. Rev.* **D**.

[29] L.N. Lipatov, Gauge invariant effective action for high-energy processes in QCD, DESY preprint 1995.

[30] L.N. Lipatov, *Zh. Eksp. Teor. Fiz.* **94**, 37 (1988); *Nucl. Phys.* **B307**, 705 (1988).

[31] M. Ademollo, A. Bellini, M. Ciafaloni, *Nucl. Phys.* **B338**, 114 (1990); *Nucl. Phys.* **B393**, 79 (1993).

[32] E. Verlinde, H. Verlinde, *Nucl. Phys.* **B371**, 246 (1992); QCD at high energies and 2-dim. field theory, preprint Princeton PUPT-1319, IASSNS-HEP 92/30 (1993).

[33] A.R. White, *Phys. Lett.* **B339**, 87 (1994); C. Coriano, A. White, Argonne preprint ANL-HEP-CP 94-79, to appear in the proceedings of Int. Symposium on Multiparticle Dynamics, Vietri sul Mare, Sept. 1994; C. Coriano, A. White, Argonne preprints ANL-HEP-PR 94-84 and ANL-HEP-PR 95-12.

[34] R. Kirschner, t-channel approach to reggeon interactions in QCD, Leipzig preprint NTZ 18 (1995), to be published in *Phys. Rev.*.

[35] Ya.Ya. Balitzki, L.N. Lipatov, V.S. Fadin, Lectures at the IV Leningrad Winter School 1979.

[36] L.N. Lipatov, *Zh. Eksp. Teor. Fiz.* **90**, 536 (1986).

[37] R. Kirschner, L.N. Lipatov, *Z. Phys.* **C45**, 477 (1990).

[38] L.N. Lipatov, *Phys. Lett.* **251B**, 284 (1990); *Phys. Lett.* **309B**, 393 (1993).

[39] R. Kirschner, *Z. Phys.* **C65**, 505 (1995); Regge asymptotics of scattering with flavour exchange in QCD, preprint DESY 94-090, to be published in *Z. Phys.*

[40] L.N. Lipatov, High-energy asymptotics of multi-colour QCD and exactly solvable lattice models, Padova preprint DFPD/93/TH/70 (1993); *Pisma Zh. Eksp. Teor. Fiz.* **59**, 596 (1994).

[41] L.D. Faddeev, G.P. Korchemski, *Phys. Lett.* **B342**, 311 (1994).

[42] V.O. Tarasov, L.A. Takhtajan, L.D. Faddeev, *TMF* **57**, 163 (1983); V.E. Korepin, N.M. Bogoliubov, A.G. Izergin, *Quantum Inverse Scattering Method and Correlation Functions*, Cambridge Univ. Press 1993.

[43] J. Bartels, preprint DESY 91-074 (1991), unpublished; *Z. Phys.* **C60**, 471 (1993); J. Bartels, M. Wüsthoff, preprint DESY 94-016 (1994).
[44] J. Bartels, A. de Roeck, M. Loewe, *Z. Phys.* **C54**, 635 (1992).
[45] K. Golec-Biernat, J. Kwieciński, A.B. Martin, P.J. Sutton, *Phys. Lett.* **B335**, 220 (1994).
[46] G. Ingelman, P. Schlein, *Phys. Lett.* **B152**, 256 (1985); A. Donnachie, P. Landshoff, *Phys. Lett.* **B191**, 309 (1987).
[47] T. Ahmed *et al.*, H1 Collaboration, DESY preprint 95-036 (1995).
[48] J.R. Forshaw, M.G. Ryskin, DESY preprint 94-245.
[49] V.S. Fadin, L.N. Lipatov, *Pisma Zh. Eksp. Teor. Fiz.* **46**, 311 (1989); *Yad. Fiz.* **50**, 1141 (1989); *Nucl. Phys.* **B406**, 259 (1993); V.S. Fadin, R. Fiore, *Phys. Lett.* **B294**, 286 (1992).
[50] A.J. Askew, J. Kwieciński, A.D. Martin, P.J. Sutton, *Phys. Rev.* **D49**, 4402 (1994).